LUND UNIVERSITY

Linear Time-Varying Systems

Modeling and Reduction

Sandberg, Henrik

2002

Document Version:
Publisher's PDF, also known as Version of record

Link to publication

Citation for published version (APA):
Sandberg, H. (2002). *Linear Time-Varying Systems: Modeling and Reduction.* [Licentiate Thesis, Department of Automatic Control]. Department of Automatic Control, Lund Institute of Technology (LTH).

Total number of authors:
1

General rights
Unless other specific re-use rights are stated the following general rights apply:
Copyright and moral rights for the publications made accessible in the public portal are retained by the authors and/or other copyright owners and it is a condition of accessing publications that users recognise and abide by the legal requirements associated with these rights.
• Users may download and print one copy of any publication from the public portal for the purpose of private study or research.
• You may not further distribute the material or use it for any profit-making activity or commercial gain
• You may freely distribute the URL identifying the publication in the public portal

Read more about Creative commons licenses: https://creativecommons.org/licenses/

Take down policy
If you believe that this document breaches copyright please contact us providing details, and we will remove access to the work immediately and investigate your claim.

LUND UNIVERSITY

PO Box 117
221 00 Lund
+46 46-222 00 00

Linear Time-Varying Systems: Modeling and Reduction

Henrik Sandberg

Department of Automatic Control
Lund Institute of Technology
Lund, November 2002

Department of Automatic Control
Lund Institute of Technology
Box 118
SE-221 00 LUND
Sweden

E-mail: henriks@control.lth.se
WWW: http://www.control.lth.se/~henriks

ISSN 0280–5316
ISRN LUTFD2/TFRT--3229--SE

©2002 by Henrik Sandberg. All rights reserved.
Printed in Sweden by Universitetstryckeriet,
Lund University, Lund 2002

Contents

Acknowledgments 7

Introduction 9
1. Background and Motivation 9
2. Outline, Contributions, and Related Publications 10
3. About Linear Systems 12
4. Future Work 17
5. References 18

1. Balanced Truncation of Linear Time-Varying Systems 21
1. Introduction 22
2. Discrete-Time Systems 24
3. Continuous-Time Systems 31
4. Balanced Realizations and Error Bounds 36
5. Input-Output Stability of Truncated Systems 45
6. A Lower Bound on the Approximation Error 47
7. Balancing Transformations and Numerical Issues 50
8. Example: Reduction of a Diesel Exhaust Catalyst Model 54
9. Conclusions 62
10. References 62
Appendix A. Proof of Theorem 3 65
Appendix B. Sampled Lyapunov Equations 66

2. Periodic Modeling of Power Systems 69
1. Introduction 70
2. Converter Modeling 71
3. Periodic Modeling of an Inverter Locomotive 77

4. Conclusions and Future Work 82
5. References 82

3. Harmonic Modeling of the Motor Side of an Inverter Locomotive 85
1. Introduction 86
2. Method 87
3. System 89
4. Analysis of the System 95
5. Conclusions and Future Work 100
6. References 100

Acknowledgments

First of all I must thank my supervisor Anders Rantzer. He continuously amazes me with his great insight and ideas. I would also like to thank my co-supervisor Björn Wittenmark for his valuable comments on the manuscript.

I would like to thank Erik Möllerstedt who served as my mentor the first year and gave me a push in the right direction. He is also the co-author of Papers 2 and 3. Andrey Ghulchak has given some very good courses at the department and they have certainly helped to improve the quality of this thesis. Andrey together with Bo Bernhardsson have also been very helpful in answering various questions of mathematical nature. Richard Murray at the Department of Control and Dynamical Systems, Caltech, served as my advisor for some very inspiring months in 2001. His encouragement is much appreciated.

Markus Meyer, Bombardier Transportation Switzerland, and Björn Westerberg, Scania, have kindly provided me with models of locomotives and exhaust catalysts.

The personnel and colleagues at the Department of Automatic Control are truly amazing. Explicitly I would like to mention Anton Cervin who provides me with new hobbies and has suggested improvements of this manuscript, my *optimal* office-mate Johan Åkesson who always keeps a happy face, and my project-mate Rasmus Olsson. Leif Andersson's LaTeX-support has been very helpful.

This work has been supported by the Swedish Research Council and the Center for Chemical Process Design and Control (CPDC).

Finally, I thank my mother, father, and sister for always being my greatest supporters, and Lena for her patience and sense of humor.

Henrik

Introduction

1. Background and Motivation

The topic of this thesis is *time-varying* systems. The bulk of the existing control theory is devoted to the study of *time-invariant* systems. The reason is of course that time-invariant systems are simpler. Everyone knows, however, that in reality almost nothing is time invariant: people get older, machines degrade, the climate changes, etc. Time-invariant *models* are still often very useful. If the time scale of the model is small compared to the life span of the modeled process, time invariance is a good assumption.

In this thesis we will study models with time scales comparable to those of ordinary time-invariant models. General time-varying systems are normally too difficult to analyze, so we will impose *linearity* on the models. We argue that *linear time-varying* systems offer a nice trade-off between model simplicity and the ability to describe the behavior of certain processes.

In the research literature one finds many references to linear time-varying systems. Most of this work is carried out on a purely theoretical level. Almost all theoretical breakthroughs for linear time-invariant systems have been followed by generalizations into the time-varying framework a couple of years later. This is important and has led to increased insight, such as the connections between H_∞-optimal control and game theory. It is harder to find good clear-cut applications of

linear time-varying modeling in the research literature. Periodic modeling of helicopters is an exception. One of the intentions of this thesis is to give some further examples where time-varying modeling can be useful.

The thesis is also devoted to model reduction. This is an old subject. Model reduction can be seen as the search for systematic methods to simplify models. To approximate a nonlinear model with a linear one is one form of model reduction that we will take a closer look at.

One needs to define what is to be considered as a simple model. This actually depends on the scientific field you work in. In control theory often the number of equations is a measure of complexity. A small number of equations significantly simplifies the search for a good controller. In fields such as modeling of chemical kinetics other measures of simplicity may be taken. One thing to consider during reduction is to preserve the internal structure of the model to maintain the physical interpretation. Also, the simplification may be dedicated to find the dominating chemical reactions. This is not the same as reducing the number of equations, but rather a simplification of the terms in the existing equations. This thesis is written in the tradition of automatic control, so linearization and reduction of the number of equations will be the main issues.

2. Outline, Contributions, and Related Publications

The thesis consists of three papers and this introduction. Below, the contributions of the papers are summarized and related publications are given.

Paper 1

Sandberg, H. and A. Rantzer (2002): "Balanced truncation of linear time-varying systems." Submitted for journal publication.

Contributions In this paper model reduction of linear time-varying systems is considered. More precisely the so-called balanced truncation procedure is studied. Balanced truncation is often used for linear time-invariant systems because of its simplicity, the existence of error

bounds and guarantees of stability for truncated models. In this paper it is shown that this also holds for balanced truncation of time-varying systems. Furthermore, the generalized method allow us to study systems where the model order changes over time. Both continuous- and discrete-time systems are considered. The method is illustrated on a diesel exhaust catalyst model.

Related Publications This paper contains and extends the material presented in

Sandberg, H. and A. Rantzer (2002a): "Balanced model reduction of linear time-varying systems." In *Proceedings of the 15th IFAC World Congress*. Barcelona, Spain.

Sandberg, H. and A. Rantzer (2002b): "Error bounds for balanced truncation of linear time-varying systems." In *Proceedings of the 41st IEEE Conference on Decision and Control*. Las Vegas, Nevada.

Paper 2

This is a corrected version of

Sandberg, H. and E. Möllerstedt (2001): "Periodic modelling of power systems." In *Proceedings of the IFAC Workshop on Periodic Systems and Control*. Cernobbio-Como, Italy.

Contributions This paper deals with periodic modeling of power systems. The key component modeled is the power converter/inverter. This is a modern power-electronic component that enables AC/DC and DC/AC conversion in a very flexible way. However, the component also generates harmonics in power networks. Interaction of harmonics (frequency coupling) can be modeled with linear time-periodic systems, and a simple framework for single-phase converters is developed. In the paper a brief example of how the converter model can be used in modeling of the net side of an inverter locomotive is given. This model is taken from [Möllerstedt and Bernhardsson, 2000], where the modeling is done in detail.

Paper 3

This is an extended version of

Sandberg, H. and E. Möllerstedt (2000): "Harmonic modeling of the motor side of an inverter locomotive." In *Proceedings of the 9th IEEE Conference on Control Applications*. Anchorage, Alaska.

Contributions This paper deals with the modeling of the motor side of an inverter locomotive. The analysis is made under steady state, and the interaction between the harmonics in inputs and outputs is represented in a Harmonic Transfer Matrix (HTM). The HTM is a compact way to represent the interaction, and can be viewed as an extension of the Bode diagram. The cross coupling of frequencies is visualized in a simple way.

Related Publications This paper is a summary of the results obtained in the Master's thesis

Sandberg, H. (1999): "Nonlinear modeling of locomotive propulsion system and control." Technical Report Masters thesis ISRN LUTFD2/TFRT–5625–SE. Department of Automatic Control, Lund Institute of Technology, Sweden.

Outline of Chapter

Section 3 contains some motivation as to why it is often sufficient to study linear approximations of nonlinear systems. It also contains a section on linearization, i.e. how to obtain linear approximations. Section 4 contains some suggestions for future work and extensions. Section 5 finally contains the references of this introductory chapter.

3. About Linear Systems

In the book "Linear Systems" from 1980 Thomas Kailath writes in the preface

> "*Linear systems have been under study for a long time, and from several different points of view, in physics, mathematics, engineering, and many other fields. But the subject is such a fundamental and deep one that there is no doubt that linear systems will continue to be an object of study for as long as one can foresee.*"

Even today when it is fairly simple to simulate complex models in computers, students still spend a fair amount of time learning about linear systems during their undergraduate/graduate education. Most subjects concerned with modeling use some sort of approximate linear analysis at some stage. As Thomas Kailath points at, the subject is fundamental and gives insights that are not possible to obtain from computer simulations solely.

By linear systems we mean systems of linear differential equations, treated in books like [Kailath, 1980; Rugh, 1996]. In particular in control theory linear systems have a central role. This is actually rather strange, regarding that essentially every natural or technical process is more or less nonlinear in nature. So why are linear systems so widely used then? One answer is that it is essentially only for this class of systems that it is possible to do extensive *analytical* analysis. For nonlinear systems one is many times forced to rely on computer simulations. As computers get faster and easier to use one might argue that this drawback is getting less important. This is true, to a certain extent. Modern modeling tools such as MODELICA[1] and MATLAB/SIMULINK[2] are today natural to use in the development of, for example, control systems. But still, if one wants to prove certain characteristics of a system, one often needs to use linear system theory to at least some degree.

Nonlinear systems can generally be locally approximated by linear systems, as will be more discussed in the next part of this section. This allow us to come to conclusions about the nonlinear behavior of a system from analysis of linear systems. In stability analysis this is utilized in the so-called *Lyapunov's first method*, see for example [Slotine and Li, 1991]. Results like this often justifies the use of linear analysis.

Linear systems are particularly useful for automatic control purposes. One reason is that systems under control normally operate close to some nominal point. For a tank of fluid, for instance, a typical control problem could be to keep the level close to some reference level. Under this assumption linear approximations typically work very well. Another reason – and an important one – is that control systems normally

[1] see [Elmqvist *et al.*, 1999] and http://www.modelica.org
[2] from The MathWorks, Inc. See http://www.mathworks.com

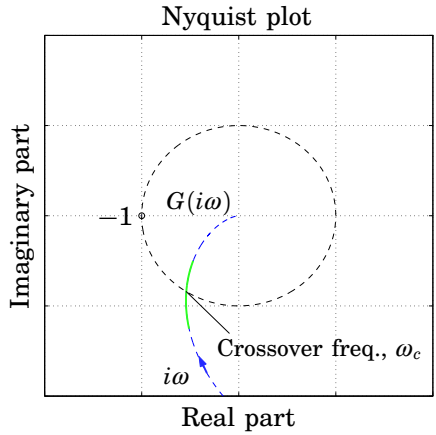

Figure 1. The Nyquist plot of a linear time-invariant system with a transfer function $G(s)$. Robustness and stability of the closed-loop system is essentially determined by how close the curve is to the point -1. If the curve is sufficiently far away the closed-loop system will work even if the true model deviates from $G(s)$. The closed-loop system is *robust*. The system behavior around the crossover frequency is most important. A partial knowledge of the system model is thus for many purposes enough for control design.

operate in closed loop, i.e. a measured output is fed back to the input. A remarkable property of feedback systems is that they, if correctly designed, become robust to model errors and can reject disturbances from the outside world.

If we have a linear model of some physical process that should be controlled, the model will normally only approximately describe the behavior of the real process. The model can though still be used for control design. How can this so often be the case? It is perhaps most simply understood with the help of the *Nyquist stability criterion*, first published in [Nyquist, 1932], and included in most basic control courses, see for example [Franklin *et al.*, 1993]. If we have a stable linear time-invariant model with the transfer function $G(s)$ the Nyquist plot can be drawn. In Figure 1 such a plot is shown. It is the distance of the curve to the point -1 that determines the stability property of the closed loop. If the controller is designed so that this distance is suffi-

ciently large the control system will work well, even if the "true" model deviates from $G(s)$. It is essentially only around the desired crossover frequency ω_c that we need to know $G(s)$ in order to design a working controller.

This was only to justify that this thesis is mainly concerned with linear systems. The thesis will not treat the synthesis of controllers. Instead we will be concerned with the steps normally taken before the synthesis in the control design process: modeling and model reduction. One should, however, notice that control design is often an iterative process and that modeling and reduction may have to be redone several times.

We will look at *time-varying* linear systems in this thesis. Often only time-invariant linear systems are meant when the word "linear system" is used. We will see, though, that by allowing time-varying parameters, we can model behavior that often is not considered to be "linear", for example, frequency coupling.

Linearization

Most physical or technical systems encountered can be modeled with differential equations, or at least with differential-algebraic equations. In physics most theories are formulated as *partial* differential equations. However, when it is time for practical computations one often has a set of *ordinary* differential equations. These take the form

$$\dot{x}(t) \equiv \frac{dx}{dt} = f(x(t), u(t), t), \quad x(t_0) = x_0 \tag{1}$$

where $x(t) \in \boldsymbol{R}^n$ is the *state* of the system. If the state at time t_0 is known and $u(t)$ is given, then we know from the theory of differential equations that there is an unique solution $x(t)$, $t > t_0$, given that f is Lipschitz-continuous in its arguments. The signal $u(t) \in \boldsymbol{R}^m$ is the input signal. The input signal is how we can influence the system from the outside world, and from a control perspective this is very essential. The role of control engineering can be seen as the art of choosing $u(t)$ such that $x(t)$ follows a given reference trajectory $x_{ref}(t)$. In practice equations of the type (1) needs to be solved by numerical ordinary differential equation solvers.

As noted before, for many purposes it is enough to study linear approximations of (1). This is particularly true if we know that the

state of the system should be in the neighborhood of some given nominal solution $x_{nom}(t)$. A linearization of the nonlinear system (1) can be performed around a nominal solution $x_{nom}(t)$ and $u_{nom}(t)$ provided that f is differentiable in its first two arguments. Denoting the deviations from $x_{nom}(t)$ with $\Delta x(t)$ and the deviations from $u_{nom}(t)$ with $\Delta u(t)$, we get the *linearization* as

$$\Delta \dot{x}(t) = \frac{\partial f}{\partial x}(x_{nom}(t), u_{nom}(t), t) \cdot \Delta x(t) + \frac{\partial f}{\partial u}(x_{nom}(t), u_{nom}(t), t) \cdot \Delta u(t)$$

or shorter

$$\Delta \dot{x}(t) = A(t) \cdot \Delta x(t) + B(t) \cdot \Delta u(t) \tag{2}$$

where $A(t) \in \boldsymbol{R}^{n \times n}$ and $B(t) \in \boldsymbol{R}^{n \times m}$. The linearization (2) is a Taylor expansion where higher order terms have been dropped. It is only valid in a neighborhood of the nominal solution. It has to be verified to see its range of applicability.

What is then so much simpler in (2) than in (1)? One simplification is that there is a closed-form solution to the linear system, namely (see [Rugh, 1996]):

$$\Delta x(t) = \Phi(t, t_0)\Delta x(t_0) + \int_{t_0}^{t} \Phi(t, s)B(s)\Delta u(s)ds \tag{3}$$

where $\Phi(t, t_0) \in \boldsymbol{R}^{n \times n}$ is the transition matrix. The transition matrix is the solution to the matrix differential equation

$$\frac{\partial}{\partial t}\Phi(t, t_0) = A(t)\Phi(t, t_0), \quad \Phi(t_0, t_0) = I_n.$$

From closed-form solutions we can make statements about the behavior of the system without solving the equations explicitly. For example, we can make statements about all possible solutions $\Delta x(t)$ for admissible inputs $\Delta u(t)$. Apart from the closed-form solutions, the linearity in the inputs and the states is very useful in many types of analyses. For example, if $\Delta x_1(t)$ and $\Delta x_2(t)$ are two solutions to (2) for the inputs $\Delta u_1(t)$ and $\Delta u_2(t)$, then $C_1 \cdot \Delta x_1(t) + C_2 \cdot \Delta x_2(t)$ is a solution for the input $C_1 \cdot \Delta u_1(t) + C_2 \cdot \Delta u_2(t)$ for any constants C_1 and C_2.

For physical systems one can often not measure the entire state vector $x(t)$. Instead we typically have some other measurements in

the system output $y(t) \in \boldsymbol{R}^p$. The output often depends on the state and the input via a map g:

$$y(t) = g(x(t), u(t), t).$$

This relation can also be linearized for differentiable maps g:

$$\Delta y(t) = \frac{\partial g}{\partial x}(x_{nom}(t), u_{nom}(t), t) \cdot \Delta x(t) + \frac{\partial g}{\partial u}(x_{nom}(t), u_{nom}(t), t) \cdot \Delta u(t)$$

or shorter

$$\Delta y(t) = C(t) \cdot \Delta x(t) + D(t) \cdot \Delta u(t) \tag{4}$$

with $C(t) \in \boldsymbol{R}^{p \times n}$ and $D(t) \in \boldsymbol{R}^{p \times m}$.

When in this thesis the word linear systems is used, one should think that this system is an approximation of some nonlinear process. Also notice that even for a time-invariant nonlinear system, the linearization will be time varying if the nominal solution, $x_{nom}(t)$ and $u_{nom}(t)$, is time varying. We need a trajectory, the nominal solution, to be able to linearize a nonlinear system. This is many times only possible to obtain from simulations. Linear analysis should be seen as a *complement* to simulations. It can never replace the need for simulations.

4. Future Work

Some suggestions for future work are given in the papers. Here some further suggestions are given.

Model Reduction In Paper 1 balanced truncation is considered. For time-invariant systems an alternative is often to use optimal Hankel-norm reduction, [Glover, 1984]. This is in a way a more rational method for model reduction, in the sense that some sort of optimality is obtained. There are interesting connections to operator theory and *Nehari's theorem*, see for example [Young, 1988].

Some work on optimal Hankel-norm reduction of time-variable systems has already been done, see [Dewilde and van der Veen, 1998]. This could be studied and compared to balanced truncation. The error

bound for balanced truncation is a factor two larger than the bound for Hankel-optimal reduction in the time-invariant case. Is this true in the time-varying case?

Synthesis In Paper 2 and 3 modeling and some analysis of linear time-periodic systems is done. With the help of the model truncation procedure proposed in Paper 1 it is possible to obtain low-order approximations of these, if needed. For low-order time-variable systems one could synthesize LQG- or H_2/H_∞-controllers, see for example [Başar and Bernhard, 1991].

Another option would be to further explore the harmonic transfer matrix in Paper 3 or its extension: the harmonic transfer function, see [Wereley, 1991; Möllerstedt, 2000]. These are generalizations of the transfer function used for time-invariant systems, and gives a frequency domain interpretation. It could be interesting to investigate the possibilities for loop shaping and lead-lag compensation using these system representations. These should allow one to develop the same engineering intuition that exists for loop shaping of time-invariant systems.

Modeling, Analysis, and Reduction The power system modeling in Paper 2 and 3 could be done in greater detail. There is not so much analysis done using the obtained models. Robustness analysis of already existing controllers could be done, for example with IQCs as described briefly in Paper 2.

The exhaust catalyst model in Paper 1 can be used to test and develop different nonlinear model reduction techniques. Is it possible to use the information the linear time-varying simplification gives to obtain a nonlinear simplification?

5. References

Başar, T. and P. Bernhard (1991): *H^∞-optimal control and related minimax design problems - A dynamic game approach*. Systems & Control: Foundations & Applications. Birkhäuser.

Dewilde, P. and A. van der Veen (1998): *Time-varying systems*

and computations. Kluwer Academic Publishers, Dordrecht, The Netherlands.

Elmqvist, H., S. E. Mattsson, and M. Otter (1999): "Modelica – a language for physical system modeling, visualization and interaction." In *Proceedings of the 1999 IEEE Symposium on Computer-Aided Control System Design*. Hawaii, USA.

Franklin, G. F., J. D. Powell, A. Emami-Naeini, and A. R. Emami-Naeini (1993): *Feedback control of dynamic systems*. Addison-Wesley.

Glover, K. (1984): "All optimal Hankel-norm approximations of linear multivariable systems and their L_∞-error bounds." *Int. J. Control*, **39**, pp. 1115–1193.

Kailath, T. (1980): *Linear systems*. Prentice Hall, Englewood Cliffs, New Jersey.

Möllerstedt, E. and B. Bernhardsson (2000): "Out of control because of harmonics - an analysis of the harmonic response of an inverter locomotive." *IEEE Control Systems Magazine*, **20:4**, pp. 70–81.

Möllerstedt, E. (2000): *Dynamic Analysis of Harmonics in Electrical Systems*. PhD thesis ISRN LUTFD2/TFRT–1060–SE, Department of Automatic Control, Lund Institute of Technology, Sweden.

Nyquist, H. (1932): "Regeneration theory." *Bell System Technical Journal*, **11**, pp. 126–147.

Rugh, W. J. (1996): *Linear system theory*. Information and system sciences series. Prentice Hall, Upper Saddle River, New Jersey.

Slotine, J. and W. Li (1991): *Applied nonlinear control*. Prentice Hall, Upper Saddle River, New Jersey.

Wereley, N. (1991): *Analysis and Control of Linear Periodically Time Varying Systems*. PhD thesis, Dept. of Aeronautics and Astronautics, MIT.

Young, N. (1988): *An introduction to Hilbert space*. Cambridge University Press, Cambridge, UK.

Paper 1

Balanced Truncation of Linear Time-Varying Systems

Henrik Sandberg and Anders Rantzer

Abstract

In this paper balancing of time-varying linear systems is studied in discrete and continuous time. Based on relatively basic calculations with time-varying Lyapunov equations/inequalities we are able to derive both upper and lower error bounds for truncated models. These results generalize well-known time-invariant formulas. The case of time-varying state dimension is considered. Input-output stability of all truncated balanced realizations is also proven. The methods are finally successfully applied to a high order model.

1. Introduction

This paper treats model reduction of time-varying linear systems. Time-varying linear systems are of interest not only for modeling of time-varying physical processes, but also because of the fact that *time-invariant* nonlinear systems can be well approximated by *time-varying* linear systems around nominal trajectories. Linear time-varying systems have attained much attention lately, see for example the survey over periodic systems in [Bittanti and Colaneri, 1999] and references therein.

Problem Statement

We will assume a linear system G is given, either in continuous or discrete time. The system should have a finite-dimensional realization with n states. The objective is to find a system $\hat{G}$ with $\hat{n}$ states that approximates G well, where $\hat{n}$ ideally should be much smaller than n. One objective is to find simple candidates $\hat{G}$ for given G and $\hat{n}$. Another objective is to find simple functions $C_1(\cdot)$ and $C_2(\cdot)$, error bounds, such that

$$C_1(\hat{n}) \leq \left\| G - \hat{G} \right\| \leq C_2(\hat{n}), \tag{1}$$

as this simplifies the selection of $\hat{G}$. The operator norm will be the induced 2-norm. Notice that we can always compute $||G - \hat{G}||$ to any wanted degree of accuracy once $\hat{G}$ is chosen. However, this is computationally expensive and involves bisection algorithms and solving time-varying Riccati-equations, see for instance [Tadmor, 1990], which is hardly something we would like to do for each candidate $\hat{G}$. So bounds of the type (1) are helpful. Moreover, we would like essential properties of the original system G, such as stability, to be preserved for each candidate $\hat{G}$.

Previous Work

To reduce the order of linear time-invariant systems, balanced truncation is often used. Balanced realizations were introduced in [Mullis and Roberts, 1976], but were first used for the purpose of model reduction in [Moore, 1981]. A sufficient condition for asymptotic stability of truncated models was later given in [Pernebo and Silverman, 1982]. Since then an error bound has been proven, [Enns, 1984; Glover, 1984], which

gives a simple bound on the worst case error between the original and truncated model and justifies the approximation. The bound was first derived for continuous-time systems, but it also holds for discrete-time systems as proven in [Al-Saggaf and Franklin, 1987]. The bound is a sum of truncated Hankel singular values and the result is now considered to be standard and is included in most courses on robust control and identification.

Balanced realization for time-varying linear systems have also received attention, see for example [Shokoohi *et al.*, 1983; Verriest and Kailath, 1983] for some early references. However, until recently no error bound has been given for the time-variable case. To obtain bounds, methods for uncertain systems could be utilized, see for example [Beck *et al.*, 1996]. However, these bounds would be conservative as the known time-variance is encapsulated in an uncertainty ball.

The first explicit error bound for balanced time-varying models, to the authors' best knowledge, was given in [Lall *et al.*, 1998] and later refined in [Lall and Beck, 2001]. There, an operator-theoretic framework was used to give bounds similar to those that apply to time-invariant models. For time-periodic linear systems bounds have been proven in [Longhi and Orlando, 1999; Varga, 2000]. There, a special form of lifting isomorphism was used.

Contributions of This Paper

In this paper we will work directly with the time-varying observability and controllability Lyapunov inequalities (linear matrix inequalities) in both continuous and discrete time. It will be seen that it is natural to allow the state-space dimension to vary in size over time. The approach will give fairly simple calculations and also in many cases stronger error bounds (1) than in the previously mentioned references. Furthermore, the method will give new results on input-output stability of the reduced models. As special cases we will recover the known results for time-invariant and periodic systems mentioned before.

The ability to vary the state-space dimension over time is not only of interest for technical reasons. In for example stiff problems, such as chemical reactions, it is frequent that in the initial phase, many complex reactions take place and that the dynamics then slows down. It is then reasonable to have a model with many states in the initial phase and then switch to a low-order model after some time. The analysis

presented will help to decide when to switch the number of states and also how much loss in accuracy a certain choice might give.

The organization of the paper is as follows. In section 2 and 3 notation for discrete and continuous-time systems will be introduced, along with two lemmas on observability and controllability. The lemmas will form the basis of the following analysis. In section 4 we will define what a balanced system is and how we, with the help of the lemmas, can attain simple upper error bounds. In section 5 input-output stability of all truncated models is proved. In section 6 a lower error bound for truncated models is given. In section 7 an example of how balanced model truncation works in practice is given. In Appendix 10 it is shown how sampling of a continuous-time system can be combined with model truncation.

2. Discrete-Time Systems

As some aspects of the calculations are simpler for discrete-time systems, we will start at that end. It should, however, be pointed out that everything presented here will later also be done for continuous-time systems.

Preliminaries and Notation

The linear systems G that we consider are assumed to have a finite-dimensional state-space realization:

$$G : \begin{cases} x(k+1) = A(k)x(k) + B(k)u(k), & x(0) = 0 \\ y(k) = C(k)x(k) + D(k)u(k) \end{cases} \tag{2}$$

with m inputs and p outputs. It will be useful to utilize time-varying state-space dimension as commented in the introduction. It is known that minimal realizations of linear systems in general have this property, see [Gohberg *et al.*, 1992]. However, it will also be a useful technical tool for reducing the order of systems where the state-space dimension originally is constant over time. Let the state-space dimension at

time k be $n(k)$. The signals and matrices then have the dimensions:

$$A(k) \in \boldsymbol{R}^{n(k+1)\times n(k)} \quad B(k) \in \boldsymbol{R}^{n(k+1)\times m} \quad x(k) \in \boldsymbol{R}^{n(k)} \quad u(k) \in \boldsymbol{R}^{m}$$
$$C(k) \in \boldsymbol{R}^{p\times n(k)} \quad D(k) \in \boldsymbol{R}^{p\times m} \quad y(k) \in \boldsymbol{R}^{p}.$$

We will assume all the matrices are real, bounded, and defined for $k \in [0, T]$. Sometimes we will have $T = +\infty$, and then the system is assumed to be stable. Notice that as the model order may vary with k, $A(k)$ is not necessarily a square matrix but rather rectangular. We could also let the number of inputs and outputs vary over time, but we avoid this for the sake of notational simplicity.

The signals will belong to the Hilbert space ℓ_2[0,T]. We will utilize the weighted Euclidean norm as defined by

$$|x(k)|_P^2 = x^T(k)P(k)x(k)$$

with a positive-definite matrix $P(k) \in \boldsymbol{R}^{n(k)\times n(k)}$, and also the weighted ℓ_2-norm

$$||x||_P^2 = \sum_{k=0}^{T} |x(k)|_P^2. \tag{3}$$

Discrete-time signals x over a time interval $[0, \infty)$ belong to $\ell_2^n[0, \infty)$ iff the norm (3) is finite for $P(k) = I$ with $T = +\infty$. If we want to emphasize that the norm is taken over the interval $[0, T]$, we will write $||x||_{P,[0,T]}$, but the interval will normally be clear from the context. Linear systems as defined in (2) can be identified with a linear operator $G : \ell_2^m[0, T] \to \ell_2^p[0, T]$. The operator is *bounded* iff the induced norm

$$||G|| = \sup_{||u||\leq 1} ||Gu||$$

is bounded. Many times we will make an upper estimate of $||G||$ by finding a constant $C(G) > 0$ such that

$$||y|| \leq C(G) \cdot ||u||$$

for all admissible u.

The system we would like to obtain, $\hat{G}$, will be called a reduced-order system. It will have the state-space dimension $\hat{n}(k)$ where $\hat{n}(k) \leq$

$n(k)$ for all k. We will construct $\hat{G}$ from a truncation of the realization of G. The following partitions will be used:

$$A(k) = \begin{bmatrix} A_{11}(k) & A_{12}(k) \\ A_{21}(k) & A_{22}(k) \end{bmatrix} \quad A_{11}(k) \in \boldsymbol{R}^{\hat{n}(k+1)\times\hat{n}(k)} \quad x(k) = \begin{bmatrix} x_1(k) \\ x_2(k) \end{bmatrix}$$
$$B(k) = \begin{bmatrix} B_1(k) \\ B_2(k) \end{bmatrix} \qquad\qquad B_1(k) \in \boldsymbol{R}^{\hat{n}(k+1)\times m}$$
$$C(k) = \begin{bmatrix} C_1(k) & C_2(k) \end{bmatrix} \qquad C_1(k) \in \boldsymbol{R}^{p\times\hat{n}(k)}.$$

If the realization (2) is chosen such that the states $x_2(k)$ are "small" in some sense, a reasonable reduced-order candidate is obtained by truncating the corresponding states:

$$\hat{G}: \begin{cases} \hat{x}(k+1) = A_{11}(k)\hat{x}(k) + B_1(k)u(k), & \hat{x}(0) = 0 \\ \hat{y}(k) = C_1(k)\hat{x}(k) + D(k)u(k), & \hat{x}(k) \in \boldsymbol{R}^{\hat{n}(k)}. \end{cases} \tag{4}$$

The auxiliary signal

$$\hat{z}(k+1) = A_{21}(k)\hat{x}(k) + B_2(k)u(k). \tag{5}$$

will naturally show up later. It is not needed to evaluate the map $\hat{G}$. $\hat{z}(k)$ has dimension $\boldsymbol{R}^{n(k)-\hat{n}(k)}$ and is defined when truncation has occurred, i.e. $\hat{n}(k) < n(k)$. As $\hat{z}$ is not necessarily defined for all k, it will be useful to collect the time points where it does exist in a set $\mathcal{T}$:

$$\mathcal{T} = \{k : \hat{z}(k) \text{ exists}\}. \tag{6}$$

Furthermore, let us define $\hat{z}(0) = 0$ if $\hat{n}(0) < n(0)$.

If the systems G and $\hat{G}$ are supposed to have a similar input-output behavior when the above truncation scheme is used, it is important that the coordinate system in the realization of G is well chosen. As we will see, such coordinate systems exist in many cases. A change in coordinate system, $x(k) = T(k)\tilde{x}(k)$, for invertible $T(k)$, will transform the realization according to

$$\begin{aligned} \{A(k),\, B(k),\, C(k),\, D(k)\} &\xrightarrow{T(k)} \{\tilde{A}(k),\, \tilde{B}(k),\, \tilde{C}(k),\, \tilde{D}(k)\} \\ &= \{T^{-1}(k+1)A(k)T(k),\, T^{-1}(k+1)B(k),\, C(k)T(k),\, D(k)\} \end{aligned} \tag{7}$$

The Observability Lyapunov Inequality

Consider the *Lyapunov observability inequality*:

$$A^T(k)Q(k+1)A(k) + C^T(k)C(k) \leq Q(k), \quad k \in [0,T]. \tag{8}$$

$Q(k)$ is often called the *observability Gramian*. The positive semidefinite solutions $Q(k)$, $k = 0 \ldots T+1$, bound the amount of energy there will be in the output for a given initial state $x(0)$ of the system G with zero input:

$$|x(T+1)|_Q^2 + ||y||_{[0,T]}^2 \leq |x(0)|_Q^2.$$

The inequality can, however, also be used to calculate the ℓ_2-norm of the difference in the outputs from G and $\hat{G}$ when both systems are driven by the same input signal. To see this, assume there is a positive semidefinite solution $Q(k)$ to (8) with the block-diagonal structure

$$Q(k) = \begin{bmatrix} Q_1(k) & 0 \\ 0 & q(k) \cdot I_{n(k)-\hat{n}(k)} \end{bmatrix} \in \boldsymbol{R}^{n(k)\times n(k)}, \quad k = 0 \ldots T+1 \tag{9}$$

and $q(k)$ scalar. Then rewrite (8) for each k in the following way:

$$\begin{bmatrix} A(k) \\ I \end{bmatrix}^T \begin{bmatrix} Q(k+1) & 0 \\ 0 & -Q(k) \end{bmatrix} \begin{bmatrix} A(k) \\ I \end{bmatrix} + C^T(k)C(k) \leq 0. \tag{10}$$

If we apply the same input signal u to (2) and (4) we obtain the trajectories x and $\hat{x}$. Use the trajectories to calculate the difference

$$X_d(k) = \begin{bmatrix} x_1(k) - \hat{x}(k) \\ x_2(k) \end{bmatrix} \in \boldsymbol{R}^{n(k)}.$$

Multiply (10) for each k from the right with $X_d(k)$ and from the left with $X_d^T(k)$. Using that

$$A(k)X_d(k) = \begin{bmatrix} x_1(k+1) - \hat{x}(k+1) \\ x_2(k+1) - \hat{z}(k+1) \end{bmatrix}, \quad C(k)X_d(k) = y(k) - \hat{y}(k),$$

and the structure of $Q(k)$ we obtain

$$\Delta \left| \begin{bmatrix} x_1(k) - \hat{x}(k) \\ x_2(k) \end{bmatrix} \right|_Q^2 - 2q(k+1)\hat{z}^T(k+1)x_2(k+1) + |\hat{z}(k+1)|_q^2 + |y(k) - \hat{y}(k)|^2 \leq 0. \tag{11}$$

The forward difference operator Δ is defined as

$$\Delta r(k) = r(k+1) - r(k).$$

on a scalar sequence $\{r(k)\}$. Now we can state the following lemma:

LEMMA 1—OBSERVABILITY
If there is a solution $Q(k)$ with the structure (9) to the Lyapunov inequality (8) on the interval $[0, T+1]$, then the solutions of (2) and (4) satisfy

(i)

$$\left|\left|\begin{bmatrix} x_1(T+1) - \hat{x}(T+1) \\ x_2(T+1) \end{bmatrix}\right|\right|_Q^2 + ||y - \hat{y}||_{[0,T]}^2 + \sum_{k\in\mathcal{T}} \left(|\hat{z}(k)|_q^2 - 2q(k)\hat{z}^T(k)x_2(k)\right) \leq 0 \quad (12)$$

where equality holds if (8) was solved with equality.

(ii) For every non-increasing positive scalar sequence $\{a(k)\}_{k=0}^T$ we have

$$||y - \hat{y}||_{a,[0,T]}^2 - \sum_{k\in\mathcal{T}} a(k-1)2q(k)\hat{z}^T(k)x_2(k) \leq 0. \quad (13)$$

Proof. (i): Sum the inequalities (11) over the interval $k = 0 \dots T$ and notice the cancelling terms.

(ii): Multiply (11) with $a(k)$ for each k, and sum over $k = 0 \dots T$. For non-increasing $a(k)$ the partially cancelling terms becomes non-negative numbers. The sum over $\mathcal{T}$ is the only sign-indefinite term, which leads to the inequality (13). □

As seen if $\mathcal{T} = \emptyset$ the difference in output is zero, as $G = \hat{G}$. All terms in (12) are necessarily non-negative except the terms $\hat{z}^T(k)x_2(k)$. These terms are the price we pay for truncating states. One might think that if the numbers $q(k)$ are small for $k \in \mathcal{T}$, $||y-\hat{y}||_2$ will be small. Indeed, if the states $x_2(k)$ are unobservable there is a solution $Q(k)$ such that $q(k) = 0$ and $||y - \hat{y}|| = 0$. Thus a small $q(k)$ could indicate that k

should be included in the set $\mathcal{T}$ and that the corresponding states $x_2(k)$ should be truncated. However, this is only true if $\hat{z}(k)$ is always small. As we do not want to calculate $\hat{z}$ explicitly each time G and $\hat{G}$ are compared, we will obtain an *a-priori* bound on the terms $\hat{z}^T(k)x_2(k)$ by a dual analysis.

The Controllability Lyapunov Inequality

Here it will be seen how far away the states in G and $\hat{G}$ can be forced with the input signal u. The following inequality will be called the *Lyapunov controllability inequality*

$$A(k)P(k)A^T(k) + B(k)B^T(k) \leq P(k+1), \quad k \in [0, T]. \tag{14}$$

$P(k)$ is often called the *controllability Gramian*. Assume there is a positive-definite block-diagonal solution to (14):

$$P(k) = \begin{bmatrix} P_{k,1} & 0 \\ 0 & p(k) \cdot I_{n(k)-\hat{n}(k)} \end{bmatrix} \in \boldsymbol{R}^{n(k)\times n(k)}, \quad k = 0 \ldots T+1 \tag{15}$$

with $p(k)$ scalar. Notice that (14) is equivalent to

$$\begin{bmatrix} A(k) & B(k) \\ I & 0 \end{bmatrix}^T \begin{bmatrix} P^{-1}(k+1) & 0 \\ 0 & -P^{-1}(k) \end{bmatrix} \begin{bmatrix} A(k) & B(k) \\ I & 0 \end{bmatrix} \leq \begin{bmatrix} 0 & 0 \\ 0 & I \end{bmatrix}. \tag{16}$$

Now, assume we apply the same input signal u to G and $\hat{G}$. We then obtain the system trajectories x and $\hat{x}$. Multiply (16) for each k with

$$X_s(k) = \begin{bmatrix} x_1(k) + \hat{x}(k) \\ x_2(k) \\ 2u(k) \end{bmatrix} \in \boldsymbol{R}^{n(k)+m}$$

from the right and with $X_s^T(k)$ from the left. Using that

$$\begin{bmatrix} A(k) & B(k) \end{bmatrix} X_s(k) = \begin{bmatrix} x_1(k+1) + \hat{x}(k+1) \\ x_2(k+1) + \hat{z}(k+1) \end{bmatrix}$$

and the structure of $P(k)$ we get

$$\Delta \left| \begin{bmatrix} x_1(k) + \hat{x}(k) \\ x_2(k) \end{bmatrix} \right|^2_{P^{-1}} + 2p^{-1}(k+1)\hat{z}^T(k+1)x_2(k+1) + |\hat{z}(k+1)|^2_{p^{-1}} \leq 4|u(k)|^2. \quad (17)$$

Now the following lemma can be stated:

LEMMA 2—CONTROLLABILITY
If there is a solution $P(k)$ to the inequality (14) with the structure (15) on the interval $[0, T+1]$ then the solutions to (2) and (4) satisfy

(i)

$$\left| \begin{bmatrix} x_1(T+1) + \hat{x}(T+1) \\ x_2(T+1) \end{bmatrix} \right|^2_{P^{-1}} + \sum_{k \in \mathcal{T}} \left(|\hat{z}(k)|^2_{p^{-1}} + 2p^{-1}(k)\hat{z}^T(k)x_2(k) \right) \leq 4||u||^2_{[0,T]}. \quad (18)$$

(ii) For every positive non-increasing scalar sequence $\{b(k)\}_{k=0}^{T}$

$$\sum_{k \in \mathcal{T}} b(k-1)2p^{-1}(k)\hat{z}^T(k)x_2(k) \leq 4||u||^2_{b,[0,T]}. \quad (19)$$

Proof. As in Lemma 1. Use (17) instead of (11). □

The lemma gives boundaries on the reachable set in the state-space for fixed amounts of input energy. Notice that when $\mathcal{T} = \varnothing$ equation (18) reduces to the well-known result

$$|x(T+1)|^2_{P^{-1}} \leq ||u||^2_{[0,T]} + |x(0)|^2_{P^{-1}},$$

as $x(k) = \hat{x}(k)$ for all k. Also notice that the sum in (19) potentially can cancel the sum in (13), namely if

$$a(k-1)q(k) = b(k-1)p^{-1}(k) \quad (20)$$

for all $k \in \mathcal{T}$. We have obtained a bound on the terms $\hat{z}^T(k)x_2(k)$ and this will be utilized section 4.

As we will utilize the truncation recursively in the following it is convenient that the realization of $\hat{G}$, $\{A_{11}(k),B_1(k),C_1(k),D(k)\}$, fulfills the Lyapunov inequalities (8) and (14), with $Q_1(k)$ and $P_1(k)$ respectively. This can be seen from straightforward calculations.

3. Continuous-Time Systems

The previous ideas in discrete time goes through in continuous time without much alternation. However, we have to be somewhat careful when the number of states change over time.

Preliminaries and Notation

The linear operator G will now operate on the Hilbert space $L_2[0,T]$, that is $G : L_2^m[0,T] \to L_2^p[0,T]$. A measurable signal x belongs to $L_2^n[0,T]$ iff the norm

$$||x||_P^2 = \int_0^T |x(t)|_P^2 \, dt$$

is finite for $P(t) = I$. The norm $||G||$ is the standard induced norm. We assume there is a finite-dimensional realization of G:

$$G : \begin{cases} \dot{x}(t) = A(t)x(t) + B(t)u(t), & x(0) = 0 \\ y(t) = C(t)x(t) + D(t)u(t) \end{cases} \tag{21}$$

The matrices and signals have the same dimensions as in discrete time, we will for now assume the state dimension is $n(t) = n$ and is constant over time. We will assume the matrices are continuous and bounded over time in all their entries. With these conditions existence and uniqueness of solutions to (21) is guaranteed, see for example [Rugh, 1996]. When the infinite time-horizon case is studied the system is assumed to be stable.

If we use the same matrix partitions as before we can define the $\hat{n}$th-order reduced-order system $\hat{G}$:

$$\hat{G}: \begin{cases} \dot{\hat{x}}(t) = A_{11}(t)\hat{x}(t) + B_1(t)u(t), \quad \hat{x}(0) = 0 \\ \hat{y}(t) = C_1(t)\hat{x}(t) + D(t)u(t). \end{cases} \tag{22}$$

The auxiliary error signal $\hat{z} \in \boldsymbol{R}^{n-\hat{n}}$ becomes

$$\hat{z}(t) = A_{21}(t)\hat{x}(t) + B_2(t)u(t). \tag{23}$$

As we assume constant state dimension for now, the set $\mathcal{T}$ is the interval $[0, T]$.

Coordinate transformations $x(t) = T(t)\tilde{x}(t)$ with a continuously differentiable $T(t)$, non-singular for all t, gives:

$$\begin{aligned} \{A(t), B(t), C(t), D(t)\} &\xrightarrow{T(t)} \{\tilde{A}(t), \tilde{B}(t), \tilde{C}(t), \tilde{D}(t)\} \\ &= \{T^{-1}(t)[A(t)T(t) - \dot{T}(t)], T^{-1}(t)B(t), C(t)T(t), D(t)\}. \end{aligned} \tag{24}$$

so that the input-output map is invariant.

The Observability Lyapunov Inequality

The *observability Lyapunov inequality* takes the form

$$Q(t)A(t) + A^T(t)Q(t) + \dot{Q}(t) + C^T(t)C(t) \leq 0 \tag{25}$$

in continuous time. We can perform the same analysis as in section 2 by noting that (25) can be written as

$$\begin{bmatrix} A(t) \\ I \end{bmatrix}^T \begin{bmatrix} 0 & Q(t) \\ Q(t) & \dot{Q}(t) \end{bmatrix} \begin{bmatrix} A(t) \\ I \end{bmatrix} + C^T(t)C(t) \leq 0. \tag{26}$$

As in section 2 we get:

LEMMA 3—OBSERVABILITY
If there is a solution $Q(t)$ with the structure (9) to the Lyapunov inequality (25) on the interval $[0, T]$, then the solutions of (21) and (22) satisfy

(i)

$$\left|\left|\begin{bmatrix} x_1(T) - \hat{x}(T) \\ x_2(T) \end{bmatrix}\right|\right|_Q^2 + ||y - \hat{y}||^2 - \int_0^T 2q(t)\hat{z}^T(t)x_2(t)dt \leq 0 \quad (27)$$

where equality holds if (25) was solved with equality.

(ii) For every non-increasing positive continuous scalar $a(t)$ we have

$$||y - \hat{y}||_a^2 - \int_0^T a(t)2q(t)\hat{z}^T(t)x_2(t)dt \leq 0. \quad (28)$$

Proof. As Lemma 1 but use (26) instead of (10). Replace summation with integration. □

The Controllability Lyapunov Inequality

The *controllability Lyaponov inequality* takes the form

$$A(t)P(t) + P(t)A^T(t) - \dot{P}(t) + B(t)B^T(t) \leq 0 \quad (29)$$

in continuous time. If there is a positive definite solution $P(t)$, (29) is equivalent to

$$\begin{bmatrix} A(t) & B(t) \\ I & 0 \end{bmatrix}^T \begin{bmatrix} 0 & P^{-1}(t) \\ P^{-1}(t) & \frac{d}{dt}P^{-1}(t) \end{bmatrix} \begin{bmatrix} A(t) & B(t) \\ I & 0 \end{bmatrix} \leq \begin{bmatrix} 0 & 0 \\ 0 & I \end{bmatrix}. \quad (30)$$

The analog to Lemma 2 becomes:

LEMMA 4—CONTROLLABILITY
If there is a solution $P(t)$ to the inequality (29) with the structure (15) on the interval $[0, T]$ then the solutions to (21) and (22) satisfy

(i)

$$\left|\left|\begin{bmatrix} x_1(T) + \hat{x}(T) \\ x_2(T) \end{bmatrix}\right|\right|_{P^{-1}}^2 + \int_0^T 2p^{-1}(t)\hat{z}^T(t)x_2(t)dt \leq 4||u||^2. \quad (31)$$

(ii) For every positive non-increasing continuous scalar $b(t)$

$$\int_0^T b(t) 2p^{-1}(t)\hat{z}^T(t)x_2(t)dt \leq 4||u||_b^2. \tag{32}$$

Proof. As Lemma 2. Use (30) instead of (16). Replace summation with integration. □

Continuous-Time Systems with Time-Varying State Dimension

It is possible to analyze systems where the state dimension varies over time, i.e. $n(t)$ takes integer values but changes over time. This will be useful in section 4 as we then do not need to distinguish between discrete- and continuous-time systems.

Assume G has n states and that $\hat{G}$ has $\hat{n}_1$ states until time t^-, and then switches to $\hat{n}_2$ states at t^+, i.e. an instant switch. The question is what to do with new states and also with the ones that disappear. Furthermore, is Lemma 3 and 4 still valid?

From t^- to t^+ the control signal u will not have time to influence the states as the input energy becomes zero on this interval of zero measure. The dynamics of the original system G becomes

$$x(t^+) = A^J x(t^-), \quad A^J = I_n,$$

i.e. nothing happens with the states. The truncated realizations $A_{11}^J \in \boldsymbol{R}^{\hat{n}_2 \times \hat{n}_1}$ become

$$\begin{aligned} A_{11}^J &= \begin{bmatrix} I_{\hat{n}_1} \\ 0 \end{bmatrix} \qquad \hat{n}_2 > \hat{n}_1 \quad \text{or} \\ A_{11}^J &= \begin{bmatrix} I_{\hat{n}_1} & 0 \end{bmatrix} \quad \hat{n}_2 < \hat{n}_1. \end{aligned} \tag{33}$$

So new states should just be initialized to zero. If there are continuous solutions $Q(t)$ and $P(t)$ to the inequalities (25) and (29) we can readily use them as solutions to the discrete-time Lyapunov equations for the jump:

$$(A^J)^T Q(t^+) A^J = Q(t^-) \quad \text{and} \quad A^J P(t^-)(A^J)^T = P(t^+) \tag{34}$$

which are fulfilled with $Q(t^-) = Q(t^+) = Q(t)$ and $P(t^-) = P(t^+) = P(t)$. For each jump we therefore get following addition to Lemma 3:

$$\left\| \begin{bmatrix} x_1(t^+) - \hat{x}(t^+) \\ x_2(t^+) \end{bmatrix} \right\|_Q^2 - \left\| \begin{bmatrix} x_1(t^-) - \hat{x}(t^-) \\ x_2(t^-) \end{bmatrix} \right\|_Q^2 + |\hat{z}(t^+)|_q^2 - 2q(t^+)\hat{z}^T(t^+)x_2(t^+) = 0, \quad (35)$$

with $\hat{x}(t^-) \in \boldsymbol{R}^{\hat{n}_1}$ and $\hat{x}(t^+) \in \boldsymbol{R}^{\hat{n}_2}$. The two first terms get canceled by the boundary terms of the integrals from the constant state modes before and after the switch in the lemma. So the only real contribution is the two last terms. For Lemma 4 the additions become

$$\left\| \begin{bmatrix} x_1(t^+) + \hat{x}(t^+) \\ x_2(t^+) \end{bmatrix} \right\|_{P^{-1}}^2 - \left\| \begin{bmatrix} x_1(t^-) + \hat{x}(t^-) \\ x_2(t^-) \end{bmatrix} \right\|_{P^{-1}}^2 + |\hat{z}(t^+)|_{p^{-1}}^2 + 2p^{-1}(t^+)\hat{z}^T(t^+)x_2(t^+) \leq 0. \quad (36)$$

Again the only real contribution is the two last terms. The remaining sign-indefinite terms

$$q(t^+)\hat{z}^T(t^+)x_2(t^+) \quad \text{and} \quad p^{-1}(t^+)\hat{z}^T(t^+)x_2(t^+)$$

can be canceled by proper choice of $a(t)$ and $b(t)$ as will be discussed in the next section.

The conclusion is that if the jump transitions (33) are used there is no real change to the results in Lemma 3 and 4 and the set $\mathcal{T}$ can be defined exactly as in the discrete-time case, eq. (6), and we may replace the integrals $\int_0^T$ in Lemma 3 and 4 by $\int_{\mathcal{T}}$.

REMARK 1—DISCONTINUITIES IN $\hat{y}$

With the proposed scheme we see that when new states are added, i.e. $\hat{n}_2 > \hat{n}_1$, $\hat{y}$ will be continuous at the switching instant as the new states are initialized to zero. Moreover $\hat{z}(t^+)$ is zero.

In the other case when $\hat{n}_2 < \hat{n}_1$, $\hat{y}$ can be discontinuous at the switching instant as states are thrown away, and then $|\hat{z}(t^+)|^2 > 0$.

□

REMARK 2—DISCONTINUOUS STATE TRANSFORMATIONS
The technique here can also be used when one, at some time instant, would like to make an instantaneous state transformation, i.e. $T(t)$ is discontinuous. Then the jump transition matrix A^J becomes the solution to

$$T(t^+)A^J = T(t^-),$$

and all the calculations in this section can be redone with this jump matrix A^J. The corresponding Lyapunov equations to (34) become

$$(A^J)^T\tilde{Q}^+(t^+)A^J = \tilde{Q}^-(t^-) \quad \text{and} \quad A^J\tilde{P}^-(t^-)(A^J)^T = \tilde{P}^+(t^+).$$

$\tilde{\cdot}^-$ and $\tilde{\cdot}^+$ denote matrices given in the coordinate systems $T(t^-)$ and $T(t^+)$, respectively. How the solutions $P(t)$ and $Q(t)$ are transformed is discussed in section 4, equation (39). □

4. Balanced Realizations and Error Bounds

The previous sections rely heavily on the ability to obtain block-diagonal solutions to the inequalities (8), (14), (25), and (29), respectively. Often this is possible to obtain. In particular if there are any solutions $P(\cdot) > 0$ and $Q(\cdot) > 0$ for all time instants in some realization of G, there exists a *balanced realization* of G where the Lyapunov inequalities take the form

$$\begin{aligned} \tilde{A}^T(k)\Sigma(k+1)\tilde{A}(k) - \Sigma(k) + \tilde{C}^T(k)\tilde{C}(k) &\le 0, \\ \tilde{A}(k)\Sigma(k)\tilde{A}^T(k) - \Sigma(k+1) + \tilde{B}(k)\tilde{B}^T(k) &\le 0 \end{aligned} \tag{37}$$

in discrete time, and in continuous time with some extra regularity conditions

$$\begin{aligned} \Sigma(t)\tilde{A}(t) + \tilde{A}^T(t)\Sigma(t) + \dot{\Sigma}(t) + \tilde{C}^T(t)\tilde{C}(t) &\le 0, \\ \tilde{A}(t)\Sigma(t) + \Sigma(t)\tilde{A}^T(t) - \dot{\Sigma}(t) + \tilde{B}(t)\tilde{B}^T(t) &\le 0. \end{aligned} \tag{38}$$

with the diagonal solution (balanced Gramians)

$$\Sigma(\cdot) = \tilde{P}(\cdot) = \tilde{Q}(\cdot) = \operatorname{diag}\{\sigma_1(\cdot), \sigma_2(\cdot), \ldots, \sigma_n(\cdot)\} > 0.$$

A linear system G with a realization fulfilling (37) or (38) with a Gramian Σ is called a *balanced system*. σ_i will be denoted as the singular value corresponding to the state x_i in a particular balanced system. Notice that it is always possible to permute the singular values in Σ. Normally one chooses to put the elements in descending order so that

$$\sigma_1(\cdot) \geq \sigma_2(\cdot) \geq \ldots \geq \sigma_n(\cdot) > 0.$$

As the singular values change in size over time it may be that the ordering must be changed at some time instants to maintain the above order. This can be done with an instantaneous coordinate transformation (permutation), see Remark 2 in section 3. However, as we will see, the ordering is not critical to our discussion. But in general it makes good sense to put small singular values last in the Σ-matrix. By defining a balanced realization with inequalities instead of equalities it becomes non-unique, and the singular values are non-unique. This was introduced in [Hinrichsen and Pritchard, 1990; Beck *et al.*, 1996] and has several appealing properties including the possibility of tighter error bounds and that every truncated realization remains balanced.

If we have solutions $Q(\cdot)$ and $P(\cdot)$ in a given coordinate system we can obtain the needed coordinate transformation $T(\cdot)$ to obtain a balanced realization. This is the topic of many papers. In discrete time see, for example, [Shokoohi and Silverman, 1987; Varga, 2000] and references therein. In continuous time we need regularity conditions on the realization to guarantee the existence of a well-behaved balancing transformation. In [Verriest and Kailath, 1983], for instance, analyticity of the realization is assumed. In [Shokoohi *et al.*, 1983; Shokoohi *et al.*, 1984] uniform observability and controllability is assumed. How in practice to obtain $T(t)$ in continuous time is not obvious, as we need $T(t)$ and also $\dot{T}(t)$ on an interval. Pointwise we can always obtain a $T(t)$ as we will see. In Section 7 this problem will be more treated.

We will not go into much detail at this point, let us just notice that under the coordinate transformation (7) and (24) the solutions to the Lyapunov inequalities transform as

$$\begin{aligned} \tilde{Q}(\cdot) &= T^T(\cdot)Q(\cdot)T(\cdot) \\ \tilde{P}(\cdot) &= T^{-1}(\cdot)P(\cdot)T^{-T}(\cdot). \end{aligned} \tag{39}$$

so that the eigenvalues of their product is invariant. Therefore we can calculate the singular values for a realization with Gramians P and Q as

$$\sigma_i^2(\cdot) = \lambda_i(P(\cdot)Q(\cdot)) = \lambda_i(\tilde{P}(\cdot)\tilde{Q}(\cdot))$$

at each time-instant and also obtain a balancing coordinate system $T(\cdot)$. As a first step towards error-bounds for truncated balanced realizations let us note that from Lemma 1 and 2 and Lemma 3 and 4 we get the following bound:

PROPOSITION 1—CANCELLING CONDITION
If the non-increasing weights $a(\cdot)$ and $b(\cdot)$ are chosen so that for all time-instants k or t in $\mathcal{T}$

$$\begin{aligned} a(k-1)q(k) &= b(k-1)p^{-1}(k) \quad \text{(Discrete time)} \\ a(t)q(t) &= b(t)p^{-1}(t) \qquad \text{(Continuous time)} \end{aligned} \tag{40}$$

then

$$\|y - \hat{y}\|_a \leq 2\,\|u\|_b\,. \tag{41}$$

Proof. Add Lemma 1 (ii) with Lemma 2 (ii) and notice that the sign-indefinite terms are canceled if $a(k)$ and $b(k)$ fulfill the above condition. Analogous in continuous time. □

Monotonous Balanced Systems

We will proceed by formulating an error bound for truncated balanced realizations which looks familiar to the well-known time-invariant result in [Enns, 1984; Glover, 1984]. We will first look at balanced systems where the singular values are monotonous in time, as this is the simplest non-time-invariant case. It is useful to group equal singular values together as this makes the error bound sharper. If there are $N(\cdot)$ unique singular values use the notation

$$\Sigma(\cdot) = \text{diag}\{\sigma_1(\cdot)I_{s_1}, \ldots, \sigma_N(\cdot)I_{s_N}\}.$$

where $s_1(\cdot) + \ldots + s_N(\cdot) = n(\cdot)$. Now the following result is easily obtained:

THEOREM 1—MONOTONOUS BALANCED SYSTEMS
Suppose the system G has a balanced realization on the interval $[0, T]$ with $\Sigma(\cdot) = \text{diag}\{\Sigma_1(\cdot), \Sigma_2(\cdot)\}$:

$$\Sigma_1(\cdot) = \text{diag}\{\sigma_1(\cdot)I_{s_1}, \ldots, \sigma_r(\cdot)I_{s_r}\}$$
$$\Sigma_2(\cdot) = \text{diag}\{\sigma_{r+1}(\cdot)I_{s_{r+1}}, \ldots, \sigma_N(\cdot)I_{s_N}\}$$

where each singular value $\sigma_i(\cdot)$, $i = r+1 \ldots N$ is either non-increasing or non-decreasing over time.

The truncated $(s_1 + \cdots + s_r)$-order system $\hat{G}$ is then balanced by $\Sigma_1(\cdot)$ and

$$\left\| G - \hat{G} \right\| \leq 2 \sum_{i=r+1}^{N} \sup_{t \in [0,T]} \sigma_i(t). \tag{42}$$

Proof. Start by removing the states with the singular value σ_N, and call this truncated system $\hat{G}_{N-1}$. Thus put $p = q = \sigma_N$. By assumption there are two possibilities: σ_N is non-increasing or non-decreasing. First consider the non-increasing case. Then choose $b(t) = \sigma_N^2(t)$ and $a(t) = 1$ in Proposition 1 ($\mathcal{T} = [0, T]$, use $a(k-1)$ and $b(k-1)$ in discrete time) and notice the cancelling condition is fulfilled. In the non-decreasing case choose $a = \sigma_N^{-2}$ and $b = 1$. It follows that

$$||y - \hat{y}_{N-1}|| \leq 2||u||_{\sigma_N^2}, \quad \text{or}$$
$$||y - \hat{y}_{N-1}||_{\sigma_N^{-2}} \leq 2||u||$$

which leads to $||G - \hat{G}_{N-1}|| \leq 2 \sup_t \sigma_N(t)$. Next notice that $\hat{G}_{N-1}$ is still balanced with the rest of Σ (Σ_{N-1}). We proceed iteratively and remove σ_{N-1} from $\hat{G}_{N-1}$, and repeat the scheme until the system $\hat{G} = \hat{G}_r$ is reached. Finally use the triangular inequality:

$$||G - \hat{G}|| = ||G - \hat{G}_{N-1} + \hat{G}_{N-1} + \ldots + \hat{G}_{r+1} - \hat{G}|| \leq 2 \sum_{i=r+1}^{N} \sup_{t \in [0,T]} \sigma_i(t).$$

□

REMARK 3—TIME-INVARIANT BALANCED SYSTEMS
For time-invariant asymptotically stable systems we can find time-invariant solutions $\Sigma(\cdot) = \Sigma$ to (37) and (38) and we then recover the well-known result in [Enns, 1984; Glover, 1984]. □

Non-Monotonous Balanced Systems

For many systems we expect the balanced Gramians $\Sigma(\cdot)$ to be non-monotonous in time. We might try to resolve this by changing the boundary conditions to the Lyapunov inequalities until a monotonous solution is found, and then use Theorem 1. In [Lall and Beck, 2001] time-invariant Gramians Σ are searched for. This may lead to good error bounds. In any case, we would still like to have a bound for non-monotonous solutions, and this will be derived in this section. The following definition will be useful:

DEFINITION 1—THE MAX-MIN RATIO OF σ
Let the singular value $\sigma(\cdot)$ be defined on the interval $\mathcal{T} = [t_0, t_f]$, and let it have M local *maximums* for $t > t_0$, located at $t_0 < t_1^{max} < \ldots < t_M^{max} \leq t_f$. Then there will be M local *minimums* so that

$$t_0 \leq t_1^{min} < t_1^{max} < \ldots < t_M^{min} < t_M^{max} \leq t_f,$$

where $\sigma(t_i^{min})$ is the local minimum immediately before $\sigma(t_i^{max})$ for $i = 1 \ldots M$. The max-min ratio of σ is defined as

$$S_{\mathcal{T}}(\sigma) = \sigma(t_0) \prod_{i=1}^{M} \frac{\sigma(t_i^{max})}{\sigma(t_i^{min})}, \qquad M > 0$$

$$S_{\mathcal{T}}(\sigma) = \sigma(t_0), \qquad M = 0.$$

□

Now we can formulate a general error-bound that applies both to monotonous and non-monotonous balanced systems.

THEOREM 2—GENERAL ERROR BOUND
Let $l(i)$ be any function that is defined for $i = 1 \ldots L$ and takes integer values in the range $1 \ldots n$, where n is the number of states in G.

The error between the balanced system G and its truncated balanced realization $\hat{G}$, where the states $x_{l(i)}$ have been truncated on the time intervals $\mathcal{T}_i$, $i = 1 \dots L$, is bounded by

$$\left\| G - \hat{G} \right\| \leq 2 \sum_{i=1}^{L} S_{\mathcal{T}_i}(\sigma_{l(i)}), \tag{43}$$

and $\hat{G}$ is balanced.

If the singular value for some other state x_k, $k \neq l(i)$, coincides with one in the sum (43), then x_k can be truncated over the same interval without inducing extra error.

Proof. Start to truncate all states with the singular value $\sigma_{l(L)}$ over $\mathcal{T}_L$, to obtain the system $\hat{G}_{L-1}$. Permute the states so that we can use Proposition 1. Then $p(\cdot) = q(\cdot) = \sigma_{l(L)}(\cdot)$. We need to find non-increasing a and b such that

$$a(\cdot)\sigma^2_{l(L)}(\cdot) = b(\cdot).$$

If $\sigma_{l(L)}$ is initially non-increasing put $b(t) = \sigma^2_{l(L)}(t)$ and $a(t) = 1$ (use $b(k-1)$ and $a(k-1)$ in discrete time). If $\sigma_{l(L)}$ reaches a local minimum at $t_1^{min} < t_f$ define $b(t) = \sigma^2_{l(L)}(t_1^{min})$ and $a(t) = \sigma^2_{l(L)}(t_1^{min})/\sigma^2_{l(L)}(t)$ for $t > t_1^{min}$. A local maximum will be reached, either at the end of the interval or before, so t_1^{max} exists. We can continue to define $a(t)$ and $b(t)$ as above, i.e. one is always constant and the other decreasing. When the whole interval $\mathcal{T}_L$ is covered we have from Proposition 1:

$$a(t_f)||y - \hat{y}_{L-1}||^2 = \inf_{t \in \mathcal{T}_L} a(t)||y - \hat{y}_{L-1}||^2 \leq 4 \sup_{t \in \mathcal{T}_L} b(t)||u||^2 = 4b(t_0)||u||^2,$$

and therefore

$$||G - \hat{G}_{L-1}|| \leq 2\sqrt{\frac{b(t_0)}{a(t_f)}} = 2S_{\mathcal{T}_L}(\sigma_{l(L)}).$$

If $\sigma_{l(L)}$ is initially non-decreasing an analogous treatment is applicable.

Finally we can continue recursively with $i = L-1 \dots 1$ and use the triangular inequality to obtain the final result, just as in Theorem 1. □

REMARK 4—LARGE MAX-MIN RATIOS
The max-min ratio may in some cases be an unnecessarily conservative bound. This is the case when $\sigma(t_i^{max})/\sigma(t_i^{min})$ is a large number. Then it is advisable to split the interval $\mathcal{T}$ into two intervals: $\mathcal{T}_1 = [t_0, t_i^{min}]$ and $\mathcal{T}_2 = [t_i^{min}, t_f]$, and truncate the state in two steps. We can always divide every time interval $\mathcal{T}$ into smaller ones so that the singular value is monotonous in each subinterval, and remove them recursively. □

EXAMPLE 1—THE MONOTONOUS CASE
Theorem 1 follows from Theorem 2. Notice that for monotonous singular values $\sigma(\cdot)$, $S_{\mathcal{T}}(\sigma) = \sup_{\mathcal{T}} \sigma(\cdot)$. So we have

$$\begin{aligned} l(1) &= r+1, & \mathcal{T}_1 &= [0,T], & S_{\mathcal{T}_1}(\sigma_{r+1}) &= \sup_{t\in\mathcal{T}_1} \sigma_{r+1}(t), \\ &\vdots & &\vdots & &\vdots \\ l(L) &= N, & \mathcal{T}_L &= [0,T], & S_{\mathcal{T}_L}(\sigma_N) &= \sup_{t\in\mathcal{T}_L} \sigma_N(t). \end{aligned}$$

□

EXAMPLE 2—CONTINUOUS-TIME SYSTEM
Assume we have a third-order balanced continuous-time system G over the time interval $[0, 1]$. The realization has the dimensions

$$A(t) \in \boldsymbol{R}^{3\times 3}, \quad B(t) \in \boldsymbol{R}^{3\times 1}, \quad C(t) \in \boldsymbol{R}^{1\times 3}$$

and the balanced Gramian is $\Sigma(t) = \mathrm{diag}\{\sigma_1(t), \sigma_2(t), \sigma_3(t)\}$, so that σ_i is the singular value of state x_i. The singular values are plotted in Figure 1. If we truncate the state x_3 over $[0, 1]$ we obtain the system $\hat{G}_2$. As σ_3 is monotonous we can use Theorem 1:

$$||G - \hat{G}_2|| \leq 2 \sup_t \sigma_3(t) = 0.8.$$

Alternatively we use Theorem 2 and get the same value

$$||G - \hat{G}_2|| \leq 2S_{[0,1]}(\sigma_3) = 2\sigma_3(0)\frac{\sigma_3(1)}{\sigma_3(0)} = 0.8.$$

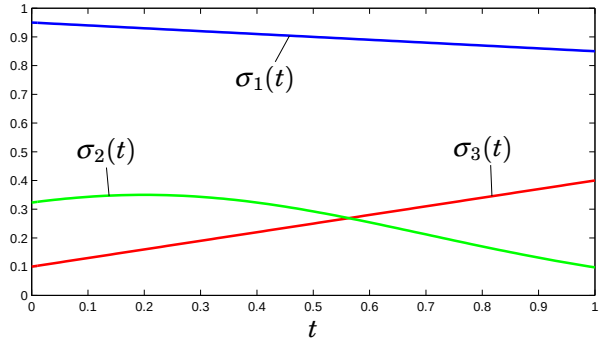

Figure 1. The singular values for Example 2. σ_2 and σ_3 are truncated in the example.

If we then want to truncate x_2 over $[0,1]$ from $\hat{G}_2$, to get $\hat{G}_1$, we have the bound

$$||\hat{G}_2 - \hat{G}_1|| \leq 2S_{[0,1]}(\sigma_2) = 2\sigma_2(0)\frac{\sigma_2(0.2)}{\sigma_2(0)} = 0.7,$$

as the only maximum is $\sigma_2(0.2)$, and the minimum immediately before is $\sigma_2(0)$. Therefore the error between the first-order system $\hat{G}_1$ and G is bounded by

$$||G - \hat{G}_1|| \leq 0.8 + 0.7 = 1.5.$$

□

As noted in Remark 4 it is important how the intervals $\mathcal{T}_i$ are chosen and how much the singular values varies over that interval. It may very well be that we need to let the state dimension vary in order for the error to be smaller than some chosen threshold.

Periodic Balanced Systems

Periodic systems are very important special cases of time-varying systems. For instance, we obtain such a system when a non-linear systems is linearized about a limit cycle. Periodic systems have realizations

where

$$A(\cdot) = A(\cdot + \omega) \qquad B(\cdot) = B(\cdot + \omega)$$
$$C(\cdot) = C(\cdot + \omega) \qquad D(\cdot) = D(\cdot + \omega)$$

for some time-period ω. These systems have received much attention in the literature, see, for instance, [Bittanti and Colaneri, 1999; Möllerstedt, 2000] and the references therein. For stable balanced periodic systems we can find periodic Gramians

$$\Sigma(\cdot) = \Sigma(\cdot + \omega)$$

which solves (37) and (38) with equality, see [Kano and Nishimura, 1996; Varga, 2000]. These solutions are clearly not monotonous. A problem with applying Theorem 2 directly to these solutions is that for each new period included in $\mathcal{T}_i$, the bound grows. Still we would like to let $t_f \to \infty$ for many periodic systems. In [Longhi and Orlando, 1999; Varga, 2000] a bound for balanced discrete-time periodic system is presented. We can also derive this bound:

COROLLARY 1—PERIODIC BALANCED DISCRETE-TIME SYSTEMS
If the balanced system G has a Gramian $\Sigma(k+\omega) = \Sigma(k)$ for all k and some ω, and $\Sigma(k)$ is partitioned as in Theorem 1, then its truncation $\hat{G}$ is balanced with $\Sigma_1(k)$ and

$$\left\| G - \hat{G} \right\| \leq 2 \sum_{k=1}^{\omega} \sum_{i=r(k)+1}^{N(k)} \sigma_i(k) \tag{44}$$

over the infinite horizon $[0, \infty)$.

Proof. Use Proposition 1. Remove first the states with the singular value $\sigma_N(1)$. As the system is periodic we can simultaneously remove these states at $1, 1+\omega, 1+2\omega, \ldots$. So $\mathcal{T} = \{1, 1+\omega, 1+2\omega, \ldots\}$. The constant values $a(k) = 1$ and $b(k) = \sigma_N^2(1)$ for all k fulfills the cancelling condition. Continue then recursively over the whole period and use then the triangular inequality. □

This might seem to be a satisfactory error bound. However, if the period is long (ω large) this bound gets large very quickly if states are removed over the whole period. In particular, if we sample a continuous-time periodic system then the bound gets less useful the faster we have

sampled the system. In the limit case, when we use the result directly on a continuous-time system, the bound is always infinity. More on sampling is given in Appendix 10.

A better technique to obtain a bound is to utilize the inequalities in (37) and (38) and to look for *time-invariant* diagonal solutions Σ. This was done in [Lall and Beck, 2001]. Solutions where only some singular values are constant over the whole period or constant for some fraction of the period is also better. It is indeed possible to find time-invariant solutions Σ in most cases. In discrete time it is always possible as is proven in [Lall and Beck, 2001]. As this methodology requires you to solve a potentially large LMI-system, we cannot consider the problem of finding good error bounds for truncation of periodic balanced systems on infinite time horizons as being fully solved.

5. Input-Output Stability of Truncated Systems

One of the advantages of the analysis so far is that it has not been necessary to worry about stability. The only thing we need is a diagonal solution $\Sigma(\cdot)$ over some interval $[0, T]$. We could for instance reduce an unstable plant over a finite interval and still get error bounds. Many balanced truncation schemes in the literature requires asymptotic stability of the plants. Still, in order for our methodology to be good, a truncated realization of a stable system G should also be stable in some sense. That this is indeed the case will be shown here in the continuous-time case. The discrete-time case is analogous. Assume from now on that there exist constants

$$0 < \underline{\sigma} \cdot I \leq \Sigma(t) \leq \overline{\sigma} \cdot I < \infty \tag{45}$$

for $0 \leq t < \infty$. From the controllability Lyapunov inequality we have

$$\begin{aligned} x^T(t)\Sigma^{-1}(t)x(t) &\leq ||u||^2_{[0,t]} \\ \hat{x}^T(t)\Sigma_1^{-1}(t)\hat{x}(t) &\leq ||u||^2_{[0,t]}. \end{aligned} \tag{46}$$

So for all $u \in L_2^m[0, \infty)$ both x and $\hat{x}$ will be bounded. Even if the states in both G and $\hat{G}$ are bounded, it is not clear that if G is input-output stable (finite L_2-gain), that $\hat{G}$ will be input-output stable. But with the results from previous sections we have the following theorem.

THEOREM 3—INPUT-OUTPUT STABILITY
If the balanced system G is input-output stable and there are constants satisfying (45), then all states x are bounded for all u in $L_2^m[0,\infty)$, and every truncated system $\hat{G}$ is also input-output stable and the states $\hat{x}$ are bounded.
Proof. See Appendix A. □

This result might seem contradictory to the result in [Pernebo and Silverman, 1982], which says that we get guaranteed asymptotic stability on $\hat{G}$ if Σ_1 and Σ_2 have no entries in common. But in the theorem above we concentrate on input-output stability. To see the effects consider the example below from [Zhou and Doyle, 1998].

EXAMPLE 3—ZHOU & DOYLE (1998)
The continuous-time system with the transfer function

$$\frac{s^2-s+2}{s^2+s+2} \quad \text{and realization} \quad \left[\begin{array}{c|c} A & B \\ \hline C & D \end{array}\right] = \left[\begin{array}{cc|c} 0 & -\sqrt{2} & 0 \\ \sqrt{2} & -1 & \sqrt{2} \\ \hline 0 & \sqrt{2} & 1 \end{array}\right]$$

is balanced with $\Sigma = I$. The $\{\sigma_2\}$-truncated system

$$\left[\begin{array}{c|c} A_{11} & B_1 \\ \hline C_1 & D \end{array}\right] = \left[\begin{array}{c|c} 0 & 0 \\ \hline 0 & 1 \end{array}\right]$$

is clearly not asymptotically stable but the pole is neither observable nor controllable, and the system is *input-output stable* and x_1 will be bounded, more precisely 0, for all u. Theorem 3 says that this will always happen when truncating a balanced system. (Obviously, in this case, a better approximation is just to keep $D = 1$, as we then get a zero-order model and the same error bound.) □

The result may seem unnecessary as we can truncate states that have equal singular values without extra cost. But the result shows that we do not need to worry about singular values that are equal for some time-instants, we will not lose input-output stability. The example also shows that a truncated system may have a non-minimal realization. The theorem, however, guarantees it is well behaved.

6. A Lower Bound on the Approximation Error

When doing optimal Hankel-norm approximation of time-invariant system a lower bound on the Hankel-norm for approximations of different system order (McMillan degree) is obtained, see [Glover, 1984; Green and Limebeer, 1995]. As the Hankel-norm always is smaller than or equal to the induced L_2-norm we also get a bound on the best possible approximation in this norm. We will see that a similar analysis is possible for linear time-varying systems. Let us consider finite-horizon linear systems G in continuous time and the following Lyapunov *equations*:

$$A^T(t)Q(t) + Q(t)A(t) - \dot{Q}(t) + C^T(t)C(t) = 0, \qquad Q(t_f) = 0 \tag{47}$$

$$A(t)P(t) + P(t)A^T(t) + \dot{P}(t) + B(t)B^T(t) = 0, \qquad P(t_0) = 0 \tag{48}$$

$$t \in (t_0, t_f): \quad P(t) > 0, \qquad Q(t) > 0. \tag{49}$$

Inequality (49) means the realization of G is completely controllable and observable. Notice that we here have dropped the Lyapunov inequalities for equalities. This is not a severe restriction. In practice one often solves the equalities as a first step anyhow, as it is less computationally expensive than solving the strict inequalities with semidefinite programming, and because it often gives good enough upper error bounds.

If we can balance the equations (47)-(49), the balanced Gramian will have the interesting property $\Sigma(t_0) = \Sigma(t_f) = 0$. Balanced finite-horizon systems of this sort were throughly studied in [Verriest and Kailath, 1983]. Among other things it was shown that if $\{A(t), B(t), C(t)\}$ are analytic functions in t, then the coordinate transformation $T(t)$ needed to obtain a balanced realization $\{\tilde{A}(t), \tilde{B}(t), \tilde{C}(t)\}$ exists, and is a Lyapunov transformation in every compact subset of (t_0, t_f). The entries of the balanced realization will tend to infinity at the boundaries t_0 and t_f. For practical computations it seems to be reasonable to embed the interval of interest, $[0, T]$, in a sufficiently large interval $[t_0, t_f]$.

Let us look at the linear system G on the time interval $[t_0, t_f]$, and divide the interval into two parts: $[t_0, \tau]$ and $[\tau, t_f]$. If we have a solution $Q(t)$ to the observability Lyapunov equation (47) we can compute the

norm $||y||_{[\tau,t_f]}$ simply if $u(t) = 0$ for $t > \tau$ and $x(\tau)$ is known. Then,

$$x^T(\tau)Q(\tau)x(\tau) = \int_\tau^{t_f} |y(t)|^2 dt = ||y||^2_{[\tau,t_f]}.$$

Analogously we have results for the controllability equation (48) and from linear optimal control theory. There is a minimum control signal $u^*(t)$ (in L_2-sense) that takes the state from $x(t_0) = 0$ to any $x(\tau)$ that fulfills

$$x^T(\tau)P^{-1}(\tau)x(\tau) = \int_{t_0}^{\tau} |u^*(t)|^2 dt = ||u^*||^2_{[t_0,\tau]},$$

see for example [Green and Limebeer, 1995]. Now define the Hankel-norm $||G||_{H,\tau}$ at time τ and calculate it as

$$||G||^2_{H,\tau} = \sup_{u\neq 0} \frac{||y||^2_{[\tau,t_f]}}{||u||^2_{[t_0,\tau]}} = \sup_{x(\tau)} \frac{x^T(\tau)Q(\tau)x(\tau)}{x^T(\tau)P^{-1}(\tau)x(\tau)} = \overline{\sigma}(P(\tau)Q(\tau))$$

where $u(t) = 0$ for $t > \tau$. As $P(\tau) > 0$ and $Q(\tau) > 0$ we can find a balancing coordinate transformation at time τ from eq. (39), so we have $\overline{\sigma}(P(\tau)Q(\tau)) = \overline{\sigma}(\Sigma^2(\tau)) = \sigma_1^2(\tau)$, because the Hankel-norm is invariant under coordinate transformations. Also notice that $||G||_{H,t_0} = ||G||_{H,t_f} = 0$ and that

$$||G||_{H,\tau} \leq ||G|| = \sup_{u\neq 0} \frac{||y||_{[t_0,t_f]}}{||u||_{[t_0,t_f]}} \tag{50}$$

for all τ in $[t_0, t_f]$. Next, define the Hankel-operator of G at time τ, $\Gamma_{G,\tau}$, as the past to future restriction of G

$$\Gamma_{G,\tau} : L_2^m[t_0,\tau] \xrightarrow{G} L_2^p[\tau,t_f].$$

We see that $||\Gamma_{G,\tau}|| = ||G||_{H,\tau}$. The operator $\Gamma_{G,\tau}$ has finite rank, namely n. We here only consider constant-state-dimensional systems as full-order systems G often come in this form. For each choice of τ there is a singular-value decomposition (Schmidt decomposition, see [Young, 1988; Green and Limebeer, 1995]) of $\Gamma_{G,\tau}$:

$$\Gamma_{G,\tau} = \sum_{i=1}^{n} \sigma_i(\tau)\langle u, v_i\rangle w_i$$

where $\{v_i\}_1^n$ is a set of orthonormal functions in $L_2^m[t_0, \tau]$ and $\{w_i\}_1^n$ is a set of orthonormal functions in $L_2^p[\tau, t_f]$. $\sigma_i(\tau) = \lambda_i^{1/2}(P(\tau)Q(\tau))$ are the singular values. $\langle \cdot, \cdot \rangle$ is the standard scalar product on $L_2^m[t_0, \tau]$:

$$\langle u, v \rangle = \int_{t_0}^{\tau} u^T(s)v(s)ds.$$

We can now state the following theorem:

THEOREM 4—LOWER ERROR BOUND
Suppose G is a linear system with a finite-horizon nth-order realization with Gramians that fulfill (47)–(49). Let the singular values be ordered so that $\sigma_1(t) \geq \ldots \geq \sigma_n(t) > 0$ for each t. Then for any linear system $\hat{G}$ of order $r < n$ it holds that

$$||G - \hat{G}||_{H,\tau} \geq \sigma_{r+1}(\tau) \tag{51}$$

for all $\tau \in [t_0, t_f]$. Furthermore,

$$||G - \hat{G}|| \geq \max_t \sigma_{r+1}(t). \tag{52}$$

Proof. The operator $\Gamma_{\hat{G},\tau}$ has rank r. If we use the Schmidt vectors v_i from $\Gamma_{G,\tau}$ as basis there exist numbers $\alpha_i \neq 0$ such that the signal $v = \sum_{i=1}^{r+1} \alpha_i v_i$ gives $\Gamma_{\hat{G},\tau} v = 0$. Now,

$$||(\Gamma_{G,\tau} - \Gamma_{\hat{G},\tau})v||^2 = ||\Gamma_{G,\tau} v||^2 = ||\sum_{i=1}^{r+1} \alpha_i \sigma_i(\tau) w_i||^2 =$$

$$\sum_{i=1}^{r+1} \alpha_i^2 \sigma_i^2(\tau) \geq \sigma_{r+1}^2(\tau) \sum_{i=1}^{r+1} \alpha_i^2 = \sigma_{r+1}^2(\tau)||v||^2.$$

This gives (51), and (50) then gives (52). □

If we make a one-step truncation ($L = 1$) of a finite-horizon balanced system G and truncate the states with the singular value $\sigma_N(t)$, we get

$$\max_t \sigma_N \leq \left\| G - \hat{G} \right\| \leq C \cdot \max_t \sigma_N$$

where $C \geq 2$ depends upon the monotonicity conditions as discussed in Theorem 2. Therefore we can many times expect a very good approximation in this type of one-step reductions. For multi-step reductions ($L > 1$) the approximation may be much less close to an optimal approximation, just as for standard balanced truncation for time-invariant systems. But notice that we have not proven that there exists an approximation that really obtains the lower bound, so we do not know exactly how far away the optimum is. In [Lall and Beck, 2001] a sufficient and necessary condition for the existence of a system $\hat{G}$ of order r for a given approximation error γ is given. The condition is however non-convex and hard to check. The discussion here only justifies the balanced truncation procedure when the lower and upper bounds are close to each other.

7. Balancing Transformations and Numerical Issues

To to use the methods in this paper in practice, we need to find diagonal solutions to Lyapunov inequalities. If we are aiming for balanced solutions, one way is to find a coordinate transformation $T(\cdot)$ for some solutions $P(\cdot)$ and $Q(\cdot)$ such that

$$\begin{aligned} \Sigma(\cdot) &= T^T(\cdot)Q(\cdot)T(\cdot) \\ \Sigma(\cdot) &= T^{-1}(\cdot)P(\cdot)T^{-T}(\cdot). \end{aligned} \tag{53}$$

Then one could apply the truncation described in this paper. In order for a coordinate transformation to be balancing, the columns in $T(\cdot)$ must be right eigenvectors of $P(\cdot)Q(\cdot)$, and the rows in $T^{-1}(\cdot)$ must be left eigenvectors of $P(\cdot)Q(\cdot)$. Furthermore, the vectors have to be scaled such that the observability and controllability Gramians not only become diagonal but also equal. Let us assume the vectors have been scaled in such a way. Later it will be seen how the scaling is dealt with. In the following we will consider the continuous-time case, as this is slightly more difficult.

Let us use the following notation for the eigenvectors

$$T(t) = \begin{bmatrix} r_1(t) & r_2(t) & \dots & r_n(t) \end{bmatrix}, \qquad r_i(t) \in \boldsymbol{R}^{n\times 1}, \tag{54}$$

$$T^{-1}(t) = \begin{bmatrix} l_1^T(t) & l_2^T(t) & \dots & l_n^T(t) \end{bmatrix}^T, \qquad l_i(t) \in \boldsymbol{R}^{1\times n}, \tag{55}$$

so that

$$P(t)Q(t)r_i(t) = \sigma_i^2(t)r_i(t)$$
$$l_i(t)P(t)Q(t) = \sigma_i^2(t)l_i(t).$$

The eigenvalues (singular values) are assumed to be ordered in descending order. For a truncated balanced system, $\hat{G}$, the elements in $\hat{x}(t) \in \boldsymbol{R}^{\hat{n}}$ are coordinates in the subspace spanned by $r_1(t), \ldots, r_{\hat{n}}(t)$, where $\sigma_1, \ldots, \sigma_{\hat{n}}$ are the largest singular values. Let us call this subspace the *dominating subspace*. We can always represent any state $\hat{x}$ in the original coordinate system by the relation:

$$\boldsymbol{R}^n \ni x(t) = \begin{bmatrix} r_1(t) & \ldots & r_{\hat{n}}(t) \end{bmatrix} \cdot \hat{x}(t) = T_{\hat{n}}(t) \cdot \hat{x}(t). \tag{56}$$

When we project the original state x onto the subspace spanned by the dominating right eigenvectors of $P(t)Q(t)$, we will loose some information in the state. The projection becomes

$$\boldsymbol{R}^{\hat{n}} \ni \hat{x}(t) = \begin{bmatrix} l_1(t) \\ \vdots \\ l_{\hat{n}}(t) \end{bmatrix} \cdot x(t) = T_{\hat{n}}^{-1}(t) \cdot x(t), \tag{57}$$

and we have

$$T_{\hat{n}}^{-1}(t)P(t)Q(t)T_{\hat{n}}(t) = \Sigma_1^2(t) = \operatorname{diag}\{\sigma_1^2(t), \ldots, \sigma_{\hat{n}}^2(t)\}.$$

The balanced truncated state-space realization of $\hat{G}$ therefore becomes

$$\hat{G} : \begin{cases} \hat{A}_B(t) = T_{\hat{n}}^{-1}(t)[A(t)T_{\hat{n}}(t) - \dot{T}_{\hat{n}}(t)] \in \boldsymbol{R}^{\hat{n}\times\hat{n}} \\ \hat{B}_B(t) = T_{\hat{n}}^{-1}(t)B(t) \in \boldsymbol{R}^{\hat{n}\times m} \\ \hat{C}_B(t) = C(t)T_{\hat{n}}(t) \in \boldsymbol{R}^{p\times\hat{n}}. \end{cases} \tag{58}$$

The subscript B is used here to emphasize that the realization is truly balanced, i.e. the corresponding Gramians are diagonal and equal.

A problem with obtaining $T(t)$ in continuous time is that there may not exist a continuously differentiable balancing transformation,

even if the singular values $\sigma_i(t)$ are continuous and differentiable. In [Shokoohi *et al.*, 1983] sufficient conditions are given for the existence of smooth balancing coordinate transformations. But even when these are fulfilled it is not obvious how to obtain a smooth transformation numerically. In [Imae *et al.*, 1992] it is instead suggested that one should find approximate balancing transformations by solving a time-varying Riccati equation. In this paper we take the somewhat "naive" approach to calculate the coordinate transformation pointwise, and a check is made afterwards to see if the obtained coordinate transformation is smooth over time. If so, a finite-difference approximation of the derivative $\dot{T}(t)$ is made. If there are isolated discontinuities in the transformation we may use jump transition matrices as discussed in Remark 2. The jump transition matrix A_{11}^J at time t_i becomes in this case:

$$\hat{x}(t_i^+) = \underbrace{T_{\hat{n}_2}^{-1}(t_i^+)T_{\hat{n}_1}(t_i^-)}_{A_{11}^J(t_i)}\hat{x}(t_i^-), \quad \hat{x}(t_i^-) \in \boldsymbol{R}^{\hat{n}_1}, \quad \hat{x}(t_i^+) \in \boldsymbol{R}^{\hat{n}_2}. \tag{59}$$

Another issue is that even for time-invariant systems it is known that if the eigenvectors are used directly as basis in the dominating subspace, it may lead to ill-conditioned numerics, as pointed out in [Safonov and Chiang, 1989]. In particular this is often the case when the sizes of the singular values differ a lot in magnitude, i.e. the case where we would benefit the most from balanced truncation as the errors are guaranteed to be small.

Choosing a Basis in the Dominating Subspace

Often it is better to use a different basis than the eigenvectors in the dominating subspace. In [Safonov and Chiang, 1989] an algorithm is given that uses arbitrary bases in the right and left eigenspaces corresponding to the dominating singular values, to compute a realization $\{\hat{A}, \hat{B}, \hat{C}\}$ for the truncated system $\hat{G}$. By using this approach there is no need to really balance the system at any time, and we can avoid potential ill-conditioned numerics.

Consider any continuously differentiable matrix $V_R(t) \in \boldsymbol{R}^{n\times\hat{n}}$ where the columns span the same subspace as the columns in $T_{\hat{n}}(t)$, and any continuously differentiable matrix $V_L^T(t) \in \boldsymbol{R}^{\hat{n}\times n}$ where the

rows span the same subspace as the rows in $T_{\hat{n}}^{-1}(t)$. We can from V_R and V_L construct a realization $\{\hat{A}, \hat{B}, \hat{C}\}$ of $\hat{G}$, i.e. a different realization of the same truncated system obtained in (58). This new realization will normally not be balanced but it will many times have good numerical properties. We here make a straightforward extension of the method in [Safonov and Chiang, 1989], so that it applies to time-varying systems. For a continuous-time system we then need a sufficiently dense time grid $\{t_k\}$.

PROCEDURE 1

1. Choose the next time point in the time grid $\{t_k\}$.
2. Compute $E(t_k) = V_L^T(t_k)V_R(t_k)$ and its singular-value decomposition $E(t_k) = U_E(t_k)S_E(t_k)V_E^T(t_k)$.
3. Let
$$S_R(t_k) = V_R(t_k)V_E(t_k)S_E^{-1/2}(t_k) \in \boldsymbol{R}^{n\times\hat{n}}$$
and
$$S_L(t_k) = V_L(t_k)U_E(t_k)S_E^{-1/2}(t_k) \in \boldsymbol{R}^{n\times\hat{n}}.$$
4. Goto 1 and iterate through the time grid.

□

Therefore $S_L^T(t)S_R(t) = I_{\hat{n}}$ and the matrix S_R is a projection that replaces $T_{\hat{n}}$ in (56). S_L^T replaces $T_{\hat{n}}^{-1}$ in (57). These are the new coordinate transformations. A realization of the truncated system $\hat{G}$ is given by

$$\hat{G}: \begin{cases} \hat{A}(t) = S_L^T(t)[A(t)S_R(t) - \dot{S}_R(t)] \in \boldsymbol{R}^{\hat{n}\times\hat{n}} \\ \hat{B}(t) = S_L^T(t)B(t) \in \boldsymbol{R}^{\hat{n}\times m} \\ \hat{C}(t) = C(t)S_R(t) \in \boldsymbol{R}^{p\times\hat{n}}. \end{cases} \tag{60}$$

After computing $S_L(t_k)$ and $S_R(t_k)$ from Procedure 1, one should check that they are smooth over time. If the time grid is sufficiently dense and all the involved matrices are smooth in t we can approximate $\dot{S}_R(t_k)$ with a finite-difference approximation. If there are discontinuities at isolated time instants t_i, or if we want to change the number of states, the jump transition matrix $A_{11}^J(t_i)$ becomes

$$A_{11}^J(t_i) = S_L^T(t_i^+)S_R(t_i^-) \in \boldsymbol{R}^{\hat{n}_2\times\hat{n}_1}, \quad \hat{x}(t_i^-) \in \boldsymbol{R}^{\hat{n}_1}, \quad \hat{x}(t_i^+) \in \boldsymbol{R}^{\hat{n}_2}.$$

If this method should improve the numerical properties of balanced truncation, we should find good bases in the left and right eigenspaces, i.e. V_L and V_R. Often orthogonal bases have good properties. In [Safonov and Chiang, 1989] a Schur decomposition of PQ is used to obtain orthogonal bases in the left and right eigenspace. This seems to be a reasonable method also for time-varying systems. With this method the columns in $S_L(t_k)$ and $S_R(t_k)$ are orthogonal.

8. Example: Reduction of a Diesel Exhaust Catalyst Model

Until now there has been no computations that show that the suggested methods really give rise to good low-order approximations in practice. In fact, there has been a fair amount of theoretical work done in the literature on time-varying balancing, but the authors have not found many real examples. Here we will give a brief overview of the results for an example, just to show that the computations are feasible.

The Linearization

We will look at a model taken from [Westerberg *et al.*, 2002]. This is a model of a diesel exhaust catalyst. At the inlet of the catalyst the exhausts from a diesel engine comes in. The exhausts are blended with some extra diesel fuel (HC). The amount of added diesel fuel is the control input in this example. In the catalyst the exhausts and the diesel react and at the outlet of the catalyst the concentration of NO_x will have decayed.

The given model consists of 28 nonlinear stiff differential equations which describe concentrations of substances and temperatures throughout the catalyst. To get a single-input single-output (SISO) system we choose the added amount of HC at the inlet as input, and the concentration of NO_2 at the outlet as output. If we are only interested in these aspects of the system, we can drop 4 of the states in the nonlinear model as these are not effected by changes in HC.

To apply the methods of this paper we need a linear system. In order to get a time-varying system we linearize the system around a

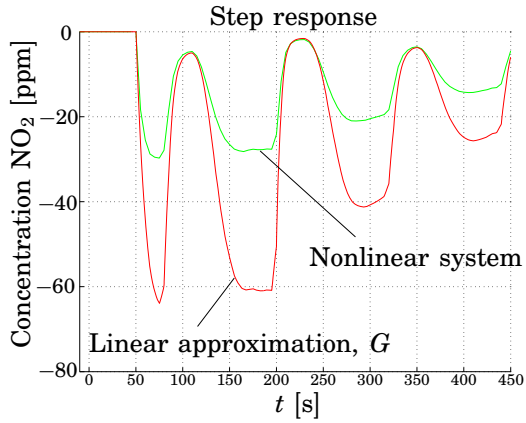

Figure 2. A step response for the diesel exhaust catalyst model. There is an increase of about 30% in the HC-injection after 50 s. The plot shows the deviation from the nominal solution. The oscillations come from the three pulses in the nominal solution. The linear approximation works well for small outputs, but there is a considerable undershoot for inputs of this magnitude. The approximation gets better the smaller the input is. As the shape of the approximation is correct, a simple gain adjustment would improve the output.

pulsating input signal (3 pulses) over a finite horizon of 460 s, so that the system does not reach steady state. We then get a time-varying linear system G with 24 states around a nominal trajectory. The linearization is made numerically so that $\{A(t), B(t), C(t)\}$ are obtained from finite-difference approximations. A step response of the linear system G and the full nonlinear system is seen in Figure 2 as a comparison. The step in u increases the input with about 30%. As seen the approximation is good for small outputs. There is a considerable undershoot in the linearization for inputs of this magnitude, smaller inputs get better approximations. But as the shape of the output of G is correct, a simple gain adjustment would improve the output. We will continue to work with the linear time-varying approximation G, as the methods in this paper apply to such systems.

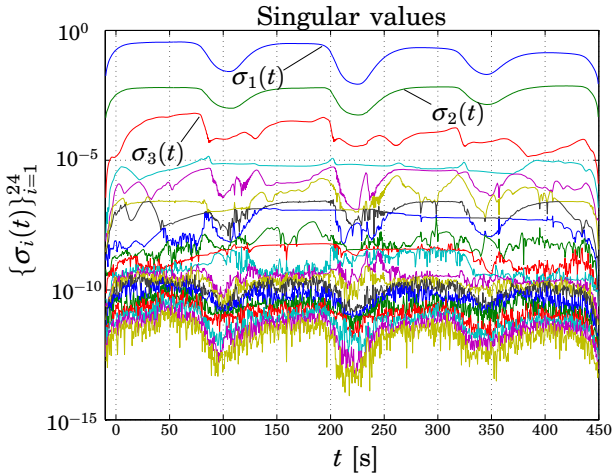

Figure 3. The singular values for the linear time-varying system G, which approximates the diesel exhaust catalyst over the time interval 0–450 s. One singular value is dominating, which predicts that one state is needed to make the approximation.

The Singular Values

To find a balanced realization and the singular values we need to solve two time-varying Lyapunov inequalities. As $n = 24$ this involves rather heavy computations. We choose to first find solutions to the system (47)–(48), with $t_0 = -10$ s and $t_f = 450$ s. The singular values, $\sigma_i(t) = \lambda_i^{1/2}(P(t)Q(t))$, are plotted in Figure 3. The plot is in logarithmic scale and we notice that one singular value, $\sigma_1(t)$, is dominating. The three pulses in the nominal input can be seen as three drops in the singular values. To reduce the computation time we have chosen the ODE-solver tolerance (for `ode15s` in MATLAB) so that only the two largest singular values have good accuracy.

Already at this stage we can get *a-priori* bounds on the error of truncated balanced realizations of G. We have shown in this paper that we can truncate balanced states that have a small singular value without inducing large errors, see Section 4. For a first-order approximation denoted by $\hat{G}_1$ ($\hat{n} = 1$), the upper error bound is essentially

$2 \cdot S_{[-10,450]}(\sigma_2)$, if we assume that the other much smaller singular values also really only have 4 maximums. Now, as $\sigma_{2,max} \approx 6 \cdot 10^{-3}$ and $\sigma_{2,min} \approx 1 \cdot 10^{-3}$ we get that $S_{[-10,450]}(\sigma_2) \approx (6 \cdot 10^{-3})^4/(1 \cdot 10^{-3})^3 = 1296 \cdot 10^{-3}$. This is an overly conservative bound. Instead one should divide into time intervals as suggested in Remark 4. So another, and better, bound is given by $2 \cdot (S_{[-10,110]} + S_{[110,225]} + S_{[225,340]} + S_{[340,450]}) \approx 2 \cdot 4 \cdot \sigma_{2,max} = 48 \cdot 10^{-3}$. As we also derived a lower bound in section 6 we can say

$$6 \cdot 10^{-3} \leq \left\| G - \hat{G}_1 \right\| \leq 48 \cdot 10^{-3}. \tag{61}$$

For a second-order truncated model denoted by $\hat{G}_2$ ($\hat{n} = 2$), it is hard to evaluate an exact bound as we have so low accuracy on $\sigma_3(t)$. But the error should be of the order 10^{-4} according to Figure 3, i.e. it should be about a factor of ten smaller than for $\hat{G}_1$.

How should one interpret these bounds? The interpretation depends on the physical meaning of the input and the output. Many times the L_2-norm does not have a direct physical meaning. But one should know that the L_2-norm is a fairly strong norm, meaning that if it is small, then many other norms will also be small. The best interpretation here is perhaps that the area between the outputs of the full-order system G and the approximations $\hat{G}$ will be very small.

The Coordinate Transformations

To find realizations for the systems $\hat{G}_1$ and $\hat{G}_2$ we use Procedure 1 outlined in Section 7. We then need a time grid $\{t_k\}$, which is chosen as the 801-point grid

$$\{t_k\} = \{0.0,\, 0.5, \ldots,\, 400.0\}.$$

We then compute orthogonal bases for the dominating right and left eigenspaces of $P(t_k)Q(t_k)$, one-dimensional for $\hat{G}_1$ and two-dimensional for $\hat{G}_2$. This is done by making Schur-factorizations for each t_k. Linear interpolation is used between the grid points.

According to the method suggested in Section 7 we should check the regularity of the coordinate transformations $S_L(t)$ and $S_R(t)$ so that they are continuously differentiable. This can be done by plotting how the lengths and the angles of the columns change over time. In this

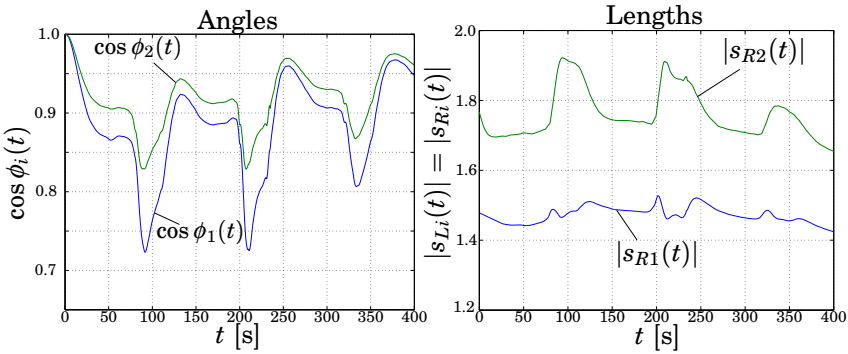

Figure 4. The evolution of the angles (left) and lengths (right) for the basis vectors in the dominating subspace used for $\hat{G}_2$. They are fairly regular and change rapidly at the time instants for the pulses in the nominal input.

case let us check the transformations for $\hat{G}_2$:

$$S_L(t) = [\, s_{L1}(t) \quad s_{L2}(t) \,] \in \boldsymbol{R}^{24\times 2}$$
$$S_R(t) = [\, s_{R1}(t) \quad s_{R2}(t) \,] \in \boldsymbol{R}^{24\times 2}.$$

Let us plot the angles $\phi_i(t)$ given by

$$s_{Ri}^T(t_0)s_{Ri}(t) = |s_{Ri}(t_0)||s_{Ri}(t)| \cos\phi_i(t).$$

and also the lengths of the columns $|s_{Ri}(t)|$ which are equal to $|s_{Li}(t)|$. These curves should look smooth if they should give rise to a coordinate transformation without any jump transition matrices. The curves are plotted in Figure 4. One sees that they are fairly regular and that no jump transitions are needed. It is interesting to notice that this is truly a time-varying coordinate transformation and that during the pulses in the nominal input the dominating two-dimensional subspace turns quickly in the 24-dimensional original state space.

The Evaluation

One should of course make some simulations of the models to see if the approximations really are good, as there are many numerical approximations in the model truncation process. In Figure 5 we see a step response test for G, $\hat{G}_1$, and $\hat{G}_2$.

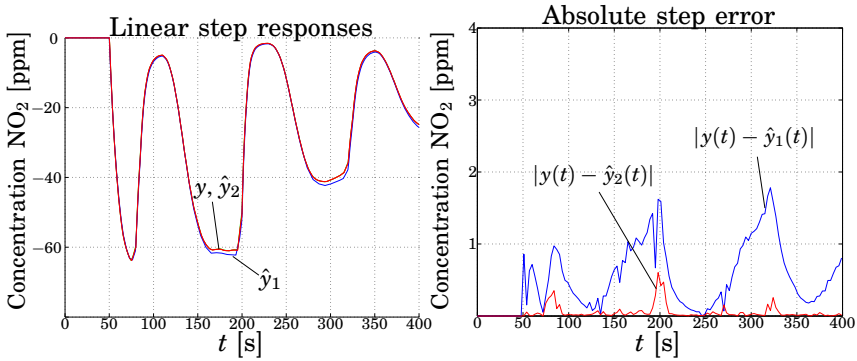

Figure 5. (Left) The step responses for the 24th-order linear time-varying system G and its first-order approximation $\hat{G}_1$, and its second-order approximation $\hat{G}_2$. (Right) The absolute errors between the responses of the systems. In this case $||y - \hat{y}_1||/||u|| = 7.2 \cdot 10^{-3}$.

The error between G and $\hat{G}_1$ in this particular case is $7.2 \cdot 10^{-3}$, which shows that a typical error is in the same order of magnitude as the worst-case bounds in (61). Notice that the step responses here are very different from what is obtained from *time-invariant* linear systems. If we instead use the second-order approximation $\hat{G}_2$, there is no visible error in the step response test.

Now we return to the original nonlinear system. As we saw in Figure 2 the only real error is the undershoot. We will use the linear model $\hat{G}_1$ and try to modify its gain to increase its accuracy. This is done by making six step responses of the nonlinear system and $\hat{G}_1$, and then we see how much the gain needs to be changed. We use spline interpolation to obtain an amplitude dependent input scaling $K(u)$. The weakly nonlinear first-order approximation becomes

$$\hat{G}_1 \cdot K(\cdot) : \begin{cases} \dot{\hat{x}}(t) = \hat{a}(t)\hat{x}(t) + \hat{b}(t)K(u(t))u(t) \\ \hat{y}(t) = \hat{c}(t)\hat{x}(t) \end{cases} \tag{62}$$

where $\{\hat{a}(t), \hat{b}(t), \hat{c}(t)\}$ is the scalar realization of $\hat{G}_1$. The functions are shown in Figure 6. Notice that the nonlinear system is not symmetric for negative and positive inputs. One would expect $K(0) \approx 1$,

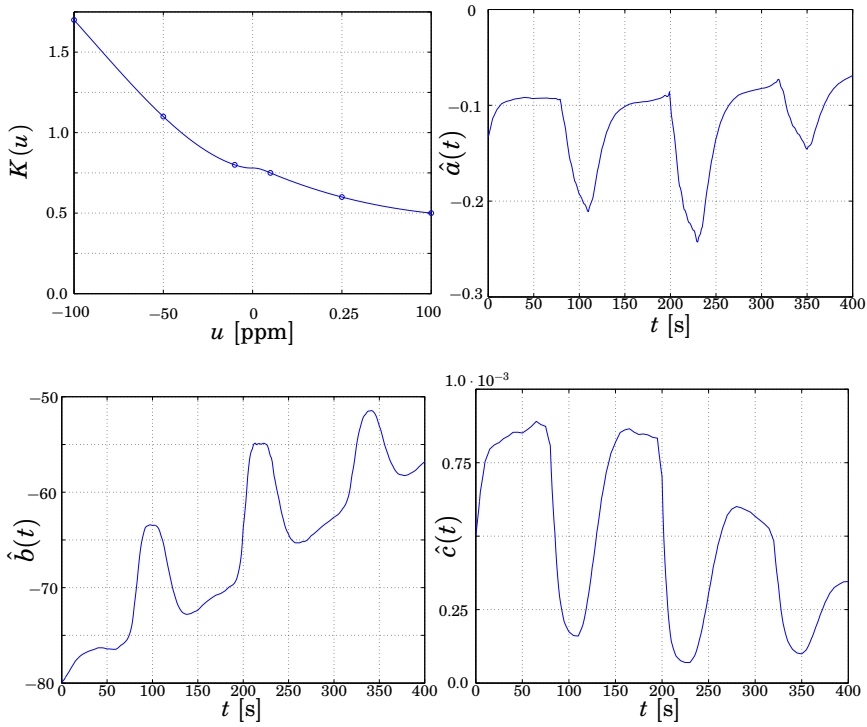

Figure 6. (Top left) The scaling $K(u)$ used to improve the accuracy of $\hat{G}_1$. Notice that it is not symmetric with respect to $u = 0$. The system is more sensitive to negative inputs. (Top right) $\hat{a}(t)$ in the realization. (Bottom left) $\hat{b}(t)$ in the realization. (Bottom right) $\hat{c}(t)$ in the realization of $\hat{G}_1$.

as linearizations typically are almost exact for small inputs. Here $K(0) \approx 0.75$. This is probably because the linearization was made with finite-difference approximations.

Next we make a test of the first-order approximation $\hat{G}_1 \cdot K(\cdot)$ and the full 24th-order nonlinear system. We apply a sine wave this time in order to see if the approximation works for different inputs than steps. In Figure 7 the input and the responses are shown. As noted the responses are very close to each other.

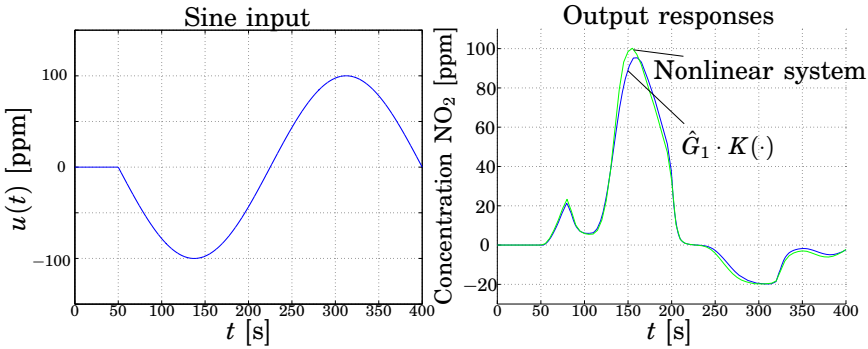

Figure 7. The responses of the full 24th-order nonlinear model and the first-order approximation $\hat{G}_1 \cdot K(\cdot)$ to a sine wave (right). The amplitude of the input is about 30% of the amplitude of the nominal input (left). The approximation must be considered as very good.

We have succeeded in finding a low-order time-varying approximation for a non-trivial high-order nonlinear system. One might ask how it can be possible to make such a low-order approximation of a complex physical system. One should then remember two things. First of all we have here only modeled the relation between injected HC and the NO_2-concentration at the outlet. The original nonlinear model describes the behavior of all concentrations and temperatures throughout the catalyst. It is to expect that the more inputs and outputs we are interested in, the more states we need in the approximation. Second, the approximation is almost linear. It is only valid in some region close to the nominal solution. One has to check for how large perturbations the model is valid by simulations like the one in Figure 7. However, it seems in this case to be quite simple to update the input scaling $K(u)$ to increase the region of validity.

The drawback of the model truncation described here is that solving for $P(t)$ and $Q(t)$ is computationally heavy, although it is feasible for n of this order of magnitude.

9. Conclusions

In this paper we have from basic analysis of the controllability and observability Lyapunov inequalities analyzed the effects of truncation of states for linear systems, in both continuous and discrete time. The analysis also covers the case when the state dimension varies over time. This is valuable as systems may need a different amount of states for different time intervals to be well approximated.

In particular we have studied balancing of time-varying systems. From the solutions to the two Lyapunov inequalities we obtain a balanced coordinate system, often well suited for truncation, and singular values. The singular values give an upper bound on the L_2-induced error for truncated models. Furthermore, we also obtained a lower error bound also expressed in the singular values. Both bounds are generalizations of well-known results for time-invariant systems.

Stability was not a main issue in the paper, as we can make approximations over a finite time horizon. Nevertheless, we proved that if a full-order system is input-output stable, then all of its truncated balanced realizations will also be input-output stable.

Finally, in an example we showed that the methods are applicable to real models. A 24th-order nonlinear model of a diesel exhaust catalyst was truncated to a first-order time-varying system with almost no error.

Future work could include finding sharper error-bounds. Especially in the infinite time-horizon case. The monotonicity conditions introduced may cause the error bound to become conservative. Furthermore, numerical issues should be considered. The requirement of solutions to the Lyapunov inequalities/equalities restricts the use of the method. For large-order systems they may be too computationally expensive to obtain.

10. References

Al-Saggaf, U. and G. Franklin (1987): "An error-bound for a discrete reduced-order model of a linear multivariable system." *IEEE Transactions on Automatic Control*, **32**, pp. 815–819.

Bamieh, B. and J. Pearson (1992): "A general framework for linear periodic systems with applications to H_∞ sampled-data control." *IEEE Transactions on Automatic Control*, **37**, pp. 418–435.

Beck, C., J. Doyle, and K. Glover (1996): "Model reduction of multidimensional and uncertain systems." *IEEE Transactions on Automatic Control*, **41:10**, pp. 1466–1477.

Bittanti, S. and P. Colaneri (1999): "Periodic control." In Webster, Ed., *Encyclopedia of Electrical and Electronics Engineering*, vol. 16, pp. 59–73. John Wiley and Sons.

Enns, D. (1984): "Model reduction with balanced realizations: an error bound and a frequency weighted generalization." In *Proceedings of the Conference on Decision and Control*. IEEE, Las Vegas, Nevada.

Glover, K. (1984): "All optimal Hankel-norm approximations of linear multivariable systems and their L_∞-error bounds." *Int. J. Control*, **39**, pp. 1115–1193.

Gohberg, I., M. Kaashoek, and L. Lerer (1992): "Minimality and realization of discrete time-varying systems." *Operator theory: Advances and Applications*, **56**, pp. 261–296.

Green, M. and D. J. Limebeer (1995): *Linear robust control*. Information and system sciences series. Prentice Hall, Englewood Cliffs, New Jersey.

Hinrichsen, D. and A. Pritchard (1990): "An improved error estimate for reduced-order models of discrete-time systems." *IEEE Transactions on Automatic Control*, **35**, pp. 317–320.

Imae, J., J. Perkins, and J. Moore (1992): "Toward time-varying balanced realization via riccati equations." *Mathematics of Control, Signals, and Systems*, **5**, pp. 313–326.

Kano, H. and T. Nishimura (1996): "A note on periodic lyapunov equations." In *Proceedings of the 35th Conference on Decision and Control*. IEEE, Kobe, Japan.

Lall, S. and C. Beck (2001): "Error bounds for balanced model reduction of linear time-varying systems." Submitted to IEEE Transactions on Automatic Control.

Lall, S., C. Beck, and G. Dullerud (1998): "Guaranteed error bounds for model reduction of linear time-varying systems." In *Proceedings of the American Control Conference*, pp. 634–638. Philadelphia, Pennsylvania.

Longhi, S. and G. Orlando (1999): "Balanced reduction of linear periodic systems." *Kybernetika*, **35:6**, pp. 737–751.

Möllerstedt, E. (2000): *Dynamic Analysis of Harmonics in Electrical Systems*. PhD thesis ISRN LUTFD2/TFRT–1060–SE, Department of Automatic Control, Lund Institute of Technology, Sweden.

Moore, B. (1981): "Principal component analysis in linear systems: controllability, observability, and model reduction." *IEEE Transactions on Automatic Control*, **26:1**, pp. 17–32.

Mullis, C. and R. Roberts (1976): "Synthesis of minimum roundoff noise fixed point digital filters." *IEEE Transactions on Circuits and Systems*, **23**, pp. 551–562.

Pernebo, L. and L. Silverman (1982): "Model reduction via balanced state space representation." *IEEE Transactions on Automatic Control*, **27**, pp. 382–387.

Rugh, W. J. (1996): *Linear system theory*. Information and system sciences series. Prentice Hall, Upper Saddle River, New Jersey.

Safonov, M. and R. Chiang (1989): "A Schur method for balanced-truncation model reduction." *IEEE Transactions on Automatic Control*, **34:7**, pp. 729–733.

Shokoohi, S., L. Silverman, and P. van Dooren (1983): "Linear time-variable systems: Balancing and model reduction." *IEEE Transactions on Automatic Control*, **28:8**, pp. 810–822.

Shokoohi, S., L. Silverman, and P. van Dooren (1984): "Linear time-variable systems: Stability of reduced models." *Automatica*, **20:1**, pp. 59–67.

Shokoohi, S. and L. M. Silverman (1987): "Identification and model reduction of time-varying discrete-time systems." *Automatica*, **23:4**, pp. 509–521.

Tadmor, G. (1990): "Input/output norms in general linear systems." *International Journal of Control*, **51:4**, pp. 911–921.

Varga, A. (2000): "Balanced truncation model reduction of periodic systems." In *Proceedings of 39th Conference on Decision and Control*. IEEE, Sydney, Australia.

Verriest, E. I. and T. Kailath (1983): "On generalized balanced realizations." *IEEE Transactions on Automatic Control*, **28:8**, pp. 833–844.

Westerberg, B., C. Künkel, and I. Odenbrand (2002): "Transient modelling of a HC-SCR catalyst for diesel exhaust aftertreatment." *Chemical Engineering Journal*. In press.

Young, N. (1988): *An introduction to Hilbert space*. Cambridge University Press, Cambridge, UK.

Zhou, K. and J. Doyle (1998): *Essentials of Robust Control*. Prentice Hall, Upper Saddle River, New Jersey.

Appendix A. Proof of Theorem 3

We will prove that input-output stability is maintained every time Proposition 1 is used to truncate a system. Under the given assumptions there are constants

$$0 < \delta_a \le a(t) \le \varepsilon_a < \infty \qquad 0 < \delta_P \le P(t) \le \varepsilon_P < \infty$$
$$0 < \delta_b \le b(t) \le \varepsilon_b < \infty \qquad 0 < \delta_Q \le Q(t) \le \varepsilon_Q < \infty$$

for all t. The calculations will be made in continuous time, but it is very similar in discrete time. Upon adding Lemma 3 (ii) and Lemma 4 (ii) we obtain

$$\left|\begin{bmatrix} x_1(T) + \hat{x}(T) \\ x_2(T) \end{bmatrix}\right|^2_{bP^{-1}} + \left|\begin{bmatrix} x_1(T) - \hat{x}(T) \\ x_2(T) \end{bmatrix}\right|^2_{aQ} + ||y - \hat{y}||^2_a \le 4||u||^2_b.$$

Using the inequality $||x + y||^2_a \ge \frac{1}{2}||x||^2_a - ||y||^2_a$ we get:

$$\frac{1}{2}|\hat{x}(T)|^2_{aq+bp^{-1}} + \frac{1}{2}||\hat{y}||^2_a \le 4||u||^2_b + ||y||^2_a + |x_1(T)|^2_{aQ_1+bP_1^{-1}} - |x_2(T)|^2_{aq+bp^{-1}}.$$

If $u \in L_2[0,\infty)$ and G is input-output stable we know that the terms $||u||_b^2$ and $||y||_a^2$ are bounded. Because of the relations (46) and $0 < aq + bp^{-1} \leq \varepsilon_a \varepsilon_Q + \varepsilon_b \delta_P^{-1} < \infty$ for all t we see that the terms involving $\hat{x}(T)$, $x_1(T)$ and $x_2(T)$ are bounded for all T. Therefore we conclude that $\hat{y} \in L_2[0,\infty)$.

Appendix B. Sampled Lyapunov Equations

In this paper we have treated systems in both discrete and continuous time. Models from physics and engineering often come in the form of differential equations. For control purposes, however, systems have to at some point be transformed into discrete time if implementation on computers is intended. We will see that this discretization can be done at the same time as the model reduction is performed.

The first step towards discretization in time is to find a different system representation. We will use so-called *lifting*, see for instance [Bamieh and Pearson, 1992]. This transformation is an isomorphic isometry, i.e. the transformation preserves the structure and the norm of the system. We will call the discretization time points $\{t(k)\}$. The inputs and the outputs of the lifted system belong to the signal spaces

$$\bar{u}(k) \in L_2^m[t(k), t(k+1)], \quad \bar{y}(k) \in L_2^p[t(k), t(k+1)], \quad \bar{x}(k) \in \boldsymbol{R}^n.$$

The lifted n-state continuous-time system G is given by

$$\begin{aligned} \bar{x}(k+1) &= \bar{A}(k)\bar{x}(k) + \bar{B}(k)\bar{u}(k) \\ \bar{y}(k) &= \bar{C}(k)\bar{x}(k) + \bar{D}(k)\bar{u}(k) \end{aligned}$$

where

$$\bar{A}(k) = \Phi(t(k+1), t(k)) \tag{63}$$

$$\bar{B}(k)\bar{u}(k) = \int_{t(k)}^{t(k+1)} \Phi(t(k+1), s) B(s) \bar{u}(k; s) ds \tag{64}$$

$$\bar{C}(k; t) = C(t)\Phi(t, t(k)) \tag{65}$$

$$\bar{D}(k)\bar{u}(k)(t) = \int_{t(k)}^{t} C(t)\Phi(t, s)B(s)\bar{u}(k; s)ds + D(t)\bar{u}(k; t), \tag{66}$$

and $\Phi(t,s)$ is the transition matrix for $\dot{x} = A(t)x$. The operators act on the following spaces

$$\begin{aligned}
&\bar{A}(k) : R^n \to R^n \\
&\bar{B}(k) : L_2^m[t(k), t(k+1)] \to R^n \\
&\bar{C}(k) : R^n \to L_2^p[t(k), t(k+1)] \\
&\bar{D}(k) : L_2^m[t(k), t(k+1)] \to L_2^p[t(k), t(k+1)].
\end{aligned}$$

We will need the adjoint operators. These act on the dual spaces. As all involved spaces are Hilbert spaces we can represent all elements in the dual space with elements in the primal space. The adjoints we need are given by

$$\bar{A}^*(k) = \Phi^T(t(k+1), t(k)) \tag{67}$$

$$\bar{B}^*(k) = B^T(t)\Phi^T(t(k+1), t) \tag{68}$$

$$\bar{C}^*(k)\bar{y}(k) = \int_{t(k)}^{t(k+1)} \Phi^T(s, t(k))C^T(s)\bar{y}(k;s)ds. \tag{69}$$

We will now see that if we have solutions to the continuous-time Lyapunov equations, $Q(t)$ and $P(t)$, we can use them at the sampling instants for the lifted system. Consider the observability Lyapunov equation in continuous time for $t \in [t(k), t(k+1)]$

$$Q(t)A(t) + A^T(t)Q(t) + \dot{Q}(t) + C^T(t)C(t) = 0$$

and its solution

$$\begin{aligned}
&\Phi^T(t(k+1), t)Q(t(k+1))\Phi(t(k+1), t) \\
&\qquad + \int_t^{t(k+1)} \Phi^T(s,t)C^T(s)C(s)\Phi(s,t)ds = Q(t).
\end{aligned} \tag{70}$$

Using the lifting operators putting $t = t(k)$, the solution (70) can be written as a discrete Lyapunov equation with the solution $Q(t(k))$:

$$\bar{A}^*(k)Q(t(k+1))\bar{A}(k) + \bar{C}^*(k)\bar{C}(k) = Q(t(k)). \tag{71}$$

We get analogous results for the controllability Lyapunov equation

$$A(t)P(t) + P(t)A^T(t) - \dot{P}(t) + B(t)B^T(t) = 0$$

with the solution

$$\Phi(t,t(k))P(t(k))\Phi^T(t,t(k)) + \int_{t(k)}^{t} \Phi(t,s)B(s)B^T(s)\Phi^T(t,s)ds = P(t) \quad (72)$$

which with the lifting operators becomes

$$\bar{A}(k)P(t(k))\bar{A}^*(k) + \bar{B}(k)\bar{B}^*(k) = P(t(k+1)). \quad (73)$$

So we can first compute continuous-time solutions $Q(t)$ and $P(t)$, and then choose suitable sampling instants $\{t(k)\}$ and compute the pointwise balancing transformation $T(t(k))$ to balance (71) and (73). Then we can truncate the lifted system and obtain error bounds as we have done before with discrete Lyapunov equations. Finally, finite-dimensional bases should be chosen to approximate the infinite-dimensional signal spaces. For instance, zero-order hold could be used for the signals $\bar{u}(k)$.

As an alternative, we could for instance first do zero-order hold sampling of the continuous-time system G and then balance the resulting discrete-time system. We would then not obtain the same approximation as above and the error bound will be in induced ℓ_2-sense, not in induced L_2-sense as in the lifting approach.

Paper 2

Periodic Modeling of Power Systems

Henrik Sandberg and Erik Möllerstedt

Abstract

This paper treats modeling of power systems with converters in a linear time-periodic framework. A power converter is a nonlinear switching device connecting an AC system to a DC system. The converter generates harmonics that might cause instabilities in systems of this kind. About a nominal periodic trajectory the power converter is well described by a periodic gain matrix, whereas the power grids often can be described by linear time-invariant models. Put together they form a linear time-periodic model. It is also shown in this paper how Integral Quadratic Constraints may be used for robustness analysis. To conclude an inverter locomotive is modeled with the described techniques.

1. Introduction

The periodicity of currents and voltages ought to make AC power systems an ideal application for linear time-periodic system theory. These systems are driven by a voltage of defined frequency and amplitude. Since only relatively small deviations from this nominal voltage are allowed, the dynamics of these systems are well captured by models which are linearized about the nominal operating trajectory. This leads to linear time-periodic (LTP) models.

However, surprisingly little periodic modeling of power systems is found in the literature. The reason for this is the following: a traditional power system consists of a number of generators connected to the grid. The generators are rotating synchronously at fundamental frequency (generally 50 or 60 Hz). The heavy generators efficiently damp all other frequencies. This means that even though harmonics exist due to nonlinearities, they are not believed to have a significant effect on the dynamics of the system. For stability analysis it is then enough to work with linear time-invariant (LTI) models which capture the dynamics of the fundamental frequency component. Harmonics are considered as a static filtering problem.

The introduction of power electronics in power systems has dramatically changed the power systems during the last decades. Power electronic devices increase the flexibility and make more optimal utilization of the grid and improved load performance possible. New concepts and solutions have emerged, like high voltage DC (HVDC) transmission and distributed power generation (DPG). The deregulation of the electricity market has further helped to make these new concepts economically viable. To allow a more optimized operation of the system, accurate methods for analysis and control design are essential. However, the switching nature of power electronics leads to systems that are much harder to analyze. Traditional analysis using LTI models is not sufficient to fully utilize the capacity of the power electronics.

Actively controlled power electronic devices like power converters, are very powerful actuators. Power flows can be changed in a fraction of a cycle. Since the grid itself is not low pass, the total system cannot be assumed to have slow dynamics. Furthermore, because of the switching dynamics, there is coupling between frequencies. Consequently, to fully utilize the possibilities brought by the power electronics, and to avoid

overly conservative solutions, harmonics and frequency coupling must be considered. For reasons of simplicity and tradition, however, LTI models that only capture the dynamics of the fundamental frequency component are still often used for the analysis.

Power systems are very large and complex. It is therefore unrealistic to model complete systems as LTP. However, LTP models are useful to understand the dynamics of power systems with switching power electronic components. In this paper it will be shown how periodic models of power systems can be used for improved analysis and control design. A power converter is used to illustrate the ideas. A related method is the so called dynamic phasors, [Stankovic *et al.*, 1999]. Related approaches to steady-state analysis of harmonic distortion in power systems are found in the literature under names like harmonic balancing, harmonic power flow studies etc. [Arrillaga *et al.*, 1994; Xu *et al.*, 1991]. However, these methods do not capture the dynamics of the system and cannot be used for stability analysis.

2. Converter Modeling

A power converter is a nonlinear coupling between two electric systems. They are often built using GTO (Gate Turn Off)-thyristors with switching frequency up to 500Hz. IGBTs (Insulated Gate Bipolar Transistors) can also be used with switching frequency up to 10kHz. Most common is that the converter is used to connect an AC system to a DC system. The AC side and DC side dynamics can generally be captured with linear time-invariant models. The problem is to obtain a good description of the coupling between the two sides, one that facilitates analysis and design of the complete system.

An Ideal Converter

An ideal single phase converter is shown in Figure 1. The ideal converter has no losses and no energy storage. The basic goal of the converter control is to shape the AC voltage so that the desired power is fed through the converter. This is done by proper switching. From Figure 1 it can be concluded that

$$v_{AC}(t) = s(t)v_{DC}(t) \tag{1}$$

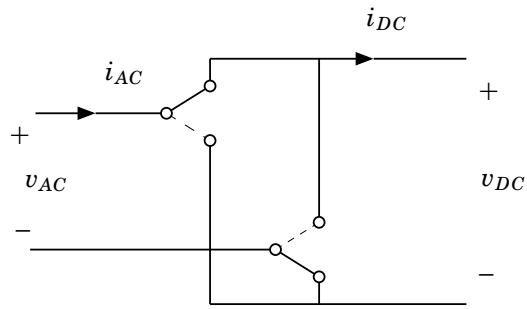

Figure 1. An ideal converter. The switches are used to control the power flow through the converter, and the reactive power generated on the AC side.

where the switch function $s(t)$ can be assigned the values 1, -1, and 0, since ideal switching is assumed. The desired AC voltage is smooth (sinusoidal), and must be approximated by using pulse width modulation, for instance.

The switch function also gives a relation between AC current and DC current:

$$i_{DC}(t) = s(t)i_{AC}(t). \tag{2}$$

Since an ideal converter has no losses and no energy storage, the instantaneous power on the DC side and the AC side must be equal, that is,

$$p_{DC}(t) = v_{DC}(t)i_{DC}(t) = v_{AC}(t)i_{AC}(t) = p_{AC}(t). \tag{3}$$

The current relation (2) can also be derived from this power balance.

In (1) and (2) v_{DC} and i_{AC} are the chosen input quantities. It would be possible to instead choose v_{AC} and i_{DC} as inputs. Which pair to choose depends on the topology of the total system. As will be seen in Section 3 the inputs to the converter are the outputs of the rest of the power system and thus the controlled variables. When modeling power systems using block diagrams the problem of choosing correct inputs and outputs always arises. It is vital that subsystems are modeled such that they are possible to interconnect. A behavioral modeling approach, as suggested by Willems [Willems, 1971], and used by equation based modeling languages like MODELICA avoids this problem, [Elmqvist *et al.*, 1999].

Linearizing the Converter

The local behavior of the converter in the neighborhood of a nominal periodic solution $\{v_{DC}^n(t),\ i_{AC}^n(t),\ s^n(t)\}$ is well described by a linear approximation of (1) and (2):

$$\begin{aligned} \Delta v_{AC}(t) &= s^n(t)\Delta v_{DC}(t) + \Delta s(t) v_{DC}^n(t) \\ \Delta i_{DC}(t) &= s^n(t)\Delta i_{AC}(t) + \Delta s(t) i_{AC}^n(t) \end{aligned} \tag{4}$$

This can be written

$$\begin{bmatrix} \Delta v_{AC}(t) \\ \Delta i_{DC}(t) \end{bmatrix} = \begin{bmatrix} 0 & s^n(t) & v_{DC}^n(t) \\ s^n(t) & 0 & i_{AC}^n(t) \end{bmatrix} \begin{bmatrix} \Delta i_{AC}(t) \\ \Delta v_{DC}(t) \\ \Delta s(t) \end{bmatrix}$$

Since the nominal solution, around which the system is linearized, is periodic, the converter is represented by a periodic gain matrix. Ideally v_{DC}^n is constant and v_{AC}^n sinusoidal of fundamental frequency. From (1) it is seen $s^n(t)$ should also be sinusoidal. However, since $s(t)$ only takes discrete values $(\pm 1, 0)$ this can only be an approximation. For three-phase systems the same approach can be taken. The AC voltage and current, as well as the switch signal are replace by vectors of the three phase quantities, $v_{AC} = [v_a\, v_b\, v_c]$, etc. Three-phase AC systems are conveniently represented in rotating coordinates, the so called $dq0$-reference frame [Kundur, 1994]. Due to the high degree of symmetry in balanced three-phase systems the effects of harmonics are often reduced.

Stability of Interconnections

Often the lines of the converter are connected to systems that are well described by linear time-invariant models (pure AC or DC systems), at least close to the nominal solution. Hence, Δi_{AC} and Δv_{DC} are obtained as

$$\begin{aligned} \Delta i_{AC} &= Y_{AC}(s)\Delta v_{AC}, \\ \Delta v_{DC} &= Z_{DC}(s)\Delta i_{DC}, \end{aligned}$$

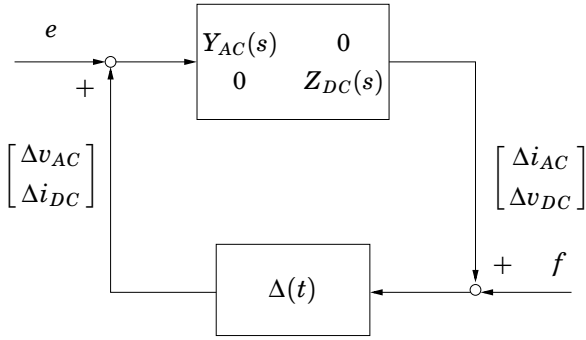

Figure 2. A feedback model of a power converter, $\Delta(t)$, that connects an AC power grid to a DC power grid. $\Delta(t)$ is here a time-periodic gain matrix given by (5) or (7).

where $Y_{AC}(s)$ is the admittance of the AC system, and $Z_{DC}(s)$ is the impedance of the DC system. The resulting closed loop is shown in Figure 2 with

$$\Delta(t) = \Delta(t+T) = \begin{bmatrix} 0 & s^n(t) \\ s^n(t) & 0 \end{bmatrix} \tag{5}$$

where T is the period of the nominal trajectory, and e and f are external noise signals. If the models of the AC/DC systems are finite dimensional, a periodic state-space model can be obtained. There are common examples of infinite dimensional systems, for example long transmission lines. However these are often approximated with finite dimensional systems.

The feedback interconnection in Figure 2 is a well-posed problem if $Z_{DC}(\infty)Y_{AC}(\infty) < 1$ and $s^n(t) \leq 1$ for all t. It is of interest to determine if the nominal solution is asymptotically stable, i.e. if all unforced solutions will converge asymptotically to the nominal solution. Once the system is written in state-space form this can be determined by Floquet-analysis, for instance. If asymptotic stability is to be determined for different $s^n(t)$ various robustness criteria can be used, for example IQCs as described in the next section.

As the system trajectories are supposed to stay close to a nominal solution, which is different for different operating conditions, a stabilizing controller is generally needed. In the simplest case let us assume the switching signal is obtained from a differentiable map $K(\cdot,\cdot)$:

$$s(t) = K(i_{AC}(t), v_{DC}(t)). \tag{6}$$

Then $\Delta s(t)$ in (4) is obtained by

$$\Delta s(t) = K^n_{i_{AC}}(t)\Delta i_{AC}(t) + K^n_{v_{DC}}(t)\Delta v_{DC}(t)$$

with

$$K^n_{i_{AC}}(t) = \frac{\partial K}{\partial i_{AC}}(i^n_{AC}(t), v^n_{DC}(t))$$
$$K^n_{v_{DC}}(t) = \frac{\partial K}{\partial v_{DC}}(i^n_{AC}(t), v^n_{DC}(t)).$$

The feedback interconnection in Figure 2 is still valid but the time-periodic block is updated by

$$\Delta(t) = \begin{bmatrix} v^n_{DC}(t)K^n_{i_{AC}}(t) & s^n(t) + v^n_{DC}(t)K^n_{v_{DC}}(t) \\ s^n(t) + i^n_{AC}(t)K^n_{i_{AC}}(t) & i^n_{AC}(t)K^n_{v_{DC}}(t) \end{bmatrix}. \tag{7}$$

Asymptotic stability and robustness of this feedback interconnection is, of course, a necessity for the power system. A static controller is a large restriction so it is vital to be able to use dynamic controllers with integral action, for instance. In the modeling example that is treated in section 3 it is shown how to include dynamic controllers and still keep much of the structure presented here.

Stability and Robustness Analysis with IQCs

To determine stability and check for robustness of the system in Figure 2 the method of Integral Quadratic Constraints (IQCs) is a valuable tool. For this analysis let us define

$$G(s) = \begin{bmatrix} Y_{AC}(s) & 0 \\ 0 & Z_{DC}(s) \end{bmatrix} \tag{8}$$

and assume it is asymptotically stable. Let $w = \Delta(t)v$ with $\Delta(t)$ defined as before. We would now like to prove asymptotic stability of the interconnection for sets of nominal periodic solutions $\{v^n_{DC}(t), i^n_{AC}(t), s^n(t)\}$, that correspond to different operating conditions of the power system. One way to do this is to give constraints on the Fourier transforms of w and v, denoted by $\hat{w}$ and $\hat{v}$, that are related by $\Delta(t)$. These constraints are formulated as

$$\int_{-\infty}^{\infty} \begin{bmatrix} \hat{v}(j\omega) \\ \hat{w}(j\omega) \end{bmatrix}^* \Pi(j\omega) \begin{bmatrix} \hat{v}(j\omega) \\ \hat{w}(j\omega) \end{bmatrix} d\omega \geq 0, \tag{9}$$

where $v, w \in L_2^2[0,\infty)$ are said to *satisfy the IQC defined by* $\Pi : jR \to C^{4\times 4}$, where $\Pi(j\omega)$ is Hermitian. The main result is as follows: if the interconnection of $G(s)$ and $\Delta(t)$ is well-posed and there exist $\varepsilon > 0$ such that

$$\begin{bmatrix} G(j\omega) \\ I \end{bmatrix}^* \Pi(j\omega) \begin{bmatrix} G(j\omega) \\ I \end{bmatrix} \leq -\varepsilon I \tag{10}$$

for all $\omega \in \boldsymbol{R}$, then the interconnection is asymptotically stable. As this is only a sufficient condition it is crucial that $\Pi(j\omega)$ is well chosen, otherwise the result can be conservative.

In [Megretski and Rantzer, 1997] the theory of IQCs is given along with a list of Π for different types of Δ. Of special interest here are those concerning time-periodic matrices. If $\Delta(t)$ satisfies several IQCs they are readily combined into a single Π giving less conservative results. In [Möllerstedt *et al.*, 2000] some numerical experiments in this direction is done to study the robustness of Distributed Power Generators (DPGs) connected to a stiff power grid.

As the nominal system here is time-periodic it would be better to include the known periodicity in G to reduce conservatism in the analysis. The original theory of IQCs however require time-invariant models $G(s)$. In [Jönsson *et al.*, 1999] an extension of the theory to handle linear time-periodic models is done. This could be utilized for the converter analysis.

EXAMPLE 1—PERIODIC SCALARS

For uncertain periodic scalars there is an IQC that gives the result in [Willems, 1971]. Signals $w = s^n(t)v$ with a T-periodic scalar $s^n(t) \leq 1$

satisfies the IQC given by

$$\Pi(j\omega) = \begin{bmatrix} X(j\omega) & Y(j\omega) \\ Y^*(j\omega) & -X(j\omega) \end{bmatrix}$$

for any

$$\begin{aligned} X(j\omega) &= X(j(\omega + 2\pi/T)) = X^*(j\omega) \geq 0 \\ Y(j\omega) &= Y(j(\omega + 2\pi/T)) = -Y^*(j\omega). \end{aligned}$$

If (5) is used as $\Delta(t)$ and we choose $X(j\omega) = \mathrm{diag}\{x_1, x_2\}$, with x_1 and x_2 non-negative scalars and $Y(j\omega) = 0$ the condition (10) becomes

$$\begin{bmatrix} x_2|Y_{AC}(j\omega)|^2 - x_1 & 0 \\ 0 & x_1|Z_{DC}(j\omega)|^2 - x_2 \end{bmatrix} \leq -\varepsilon I \qquad (11)$$

for all $\omega \in \boldsymbol{R}$ and some $\varepsilon > 0$. If we choose $x_1 = x_2 = 1$ this is just the small-gain theorem. If $Y_{AC}(s)$ and $Z_{DC}(s)$ are known we might however find $(j2\pi/T)$-periodic $x_1(j\omega)$ and $x_2(j\omega)$ that satisfies (11), and thereby proving stability of the interconnection in Figure 2 for *every* nominal T-periodic $s^n(t)$. □

3. Periodic Modeling of an Inverter Locomotive

In this section it is shown that periodic modeling of a fairly complex power system is indeed possible, and also provides with more information than a linear time-invariant approach would have done. Here an inverter locomotive is studied, schematically illustrated in Figure 3, with two power converters connected via a DC-link, a so-called back-to-back configuration. This is a common solution in modern variable-speed drives. It offers great flexibility. For example, it can operate on different power grids and be used to minimize the reactive power on the grid. However, this type of locomotive has been involved in instabilities on the power net, as in Zürich 1995 [Meyer, 1999a], which makes it an interesting modeling object. Some of the problems are believed to be due to the creation of harmonics in the power converters of

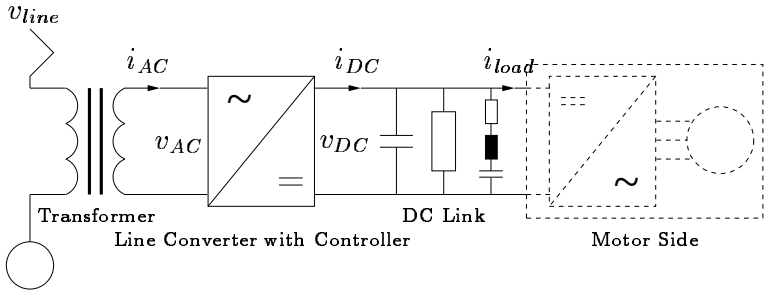

Figure 3. A schematic figure of an inverter locomotive. The locomotive consists of a transformer, a line converter, a DC-link, and the motor side. The construction opens new possibilities for control, and for operating the same locomotive on different power grids, which simplifies border crossing.

the locomotives. Such effects should be captured in a periodic model. In [Möllerstedt and Bernhardsson, 2000] the locomotive modeling was done in detail. Here those results will be summarized and it will be shown how the model fits into the framework of Section 2.

The line converter is used to keep the DC-link voltage level constant and to draw a sinusoidal current of correct frequency and phase from the grid. By controlling the shape of i_{AC} the locomotive can be used to compensate for reactive power on the net. The equations (1) and (2) describe the relation between the transformer and the link. Ideally i_{DC} would be constant but from (2) it is seen that it equals the product of two sinusoids and thus a strong harmonic of twice the grid frequency is present. This frequency is damped by a passive filter in the link. The link also contains a large capacitor to stabilize the voltage level of the link. Here the link is modeled by a third-order impedance

$$Z_{DC}(s) = -\frac{C_f L_f s^2 + C_f R_f s + 1}{(C_f L_f s^2 + C_f R_f s + 1)(Cs + 1/R) + C_f s}$$

where C is the capacitance of the large capacitor, R is the resistance of the link, and C_f, L_f, and R_f belong to the passive filter. Now $v_{DC} = Z_{DC}(s)(i_{load} - i_{DC})$. The transformer that is connected to the other side

of the converter is modeled with the admittance

$$Y_{AC}(s) = \frac{1}{sL_{tr} + R_{tr}}$$

with L_{tr} and R_{tr} being the inductance and resistance of the transformer. The model of the AC side becomes $i_{AC} = Y_{AC}(s)(v_{line} - v_{AC})$.

There is a second converter in the locomotive used to generate three-phase AC of variable frequency to control an asynchronous engine. The symmetry in the three-phase arrangement reduces the harmonics from the engine. With the so called $dq0$-transformation, mentioned before, this side can be modeled as an LTI system. Here the motor side will be replaced by a current sink, i_{load} =constant. This is a fairly good approximation of a three-phase engine running in steady state, as it then requires constant instantaneous power. In [Sandberg and Möllerstedt, 2000] modeling of the motor side of an inverter locomotive is done.

To get a linear time-periodic model a periodic trajectory of the system is needed. For complex systems this is done by first simulating the entire system. Here the periodic trajectory will have a frequency of $16 + 2/3$Hz (the grid frequency). $i^n_{AC}(t)$ and $s^n(t)$ are sinusoids, and v^n_{DC} and i_{load} are constant. The linearized model can be put together as in Figure 4 with

$$\Delta(t) = \begin{bmatrix} 0 & s^n(t) & v^n_{DC}(t) \\ s^n(t) & 0 & i^n_{AC}(t) \end{bmatrix} \tag{12}$$

and $G(s)$ containing $Z_{DC}(s)$ and $Y_{AC}(s)$ as before. Notice $\Delta(t)$ now has one more input that comes from a possibly dynamic controller. The loop now contains the normal control system blocks: the controller, the actuator (the converter), and the process (the transformer and the link).

As $G(s)$ and $\Delta(t)$ can be assembled into a linear time-periodic state-space model standard techniques can be used to design a local controller about the nominal trajectory. Here however, a global controller is just taken from [Möllerstedt and Bernhardsson, 2000], is linearized and put into the loop to allow us to do some analysis. The controller contains a PI-controller, a model of the transformer and a simple model of the pulse width modulation used to get $s(t)$.

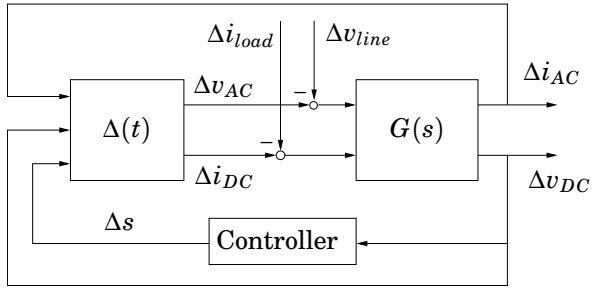

Figure 4. A block diagram of the linearized inverter locomotive with a converter controller trying to keep v_{DC} constant. The converter model, a time-periodic matrix $\Delta(t)$, is here given by (12).

With this model different types of linear analysis can be made. For example, with the Nyquist stability criterion for linear periodic systems presented in [Wereley, 1991], a gain margin for the PI-controller is obtainable. Simulations verify that this predicted stability margin actually is very close to the real one, see [Möllerstedt and Bernhardsson, 2000] for details. Analysis like this is valuable as simulations can only give a simple yes/no answer to the stability question. With stability margins, bounds on acceptable component parameters in the link can be obtained. This is useful as parameters of electrical components always are uncertain to some degree.

To study stability of interconnections of several locomotives the admittance of each locomotive is needed. Admittance is here defined to be the influence of the grid voltage (Δv_{line}) on the drawn current (Δi_{AC}). Often this relation is modeled with a time-invariant system, see [Meyer, 1999a]. By plotting how harmonics interact in the periodic locomotive model we derived above, we can see if this would be possible in this case. In Figure 5 the interaction is visualized for two different operating conditions of a locomotive. The main diagonal is essentially the amplitude part of a Bode plot, i.e. amplification of a frequency. The sub-diagonals show the transfer from one frequency to another. The shift in these cases is twice the grid frequency, 33+1/3Hz. The sub-diagonals are considerably large in both cases and even contain resonance peaks. Thus to design controllers based only on time-invariant

models (essentially the main diagonals) leads to either unsafe or overly conservative solutions in this case. The analysis of interconnections of several locomotive models remains to be done.

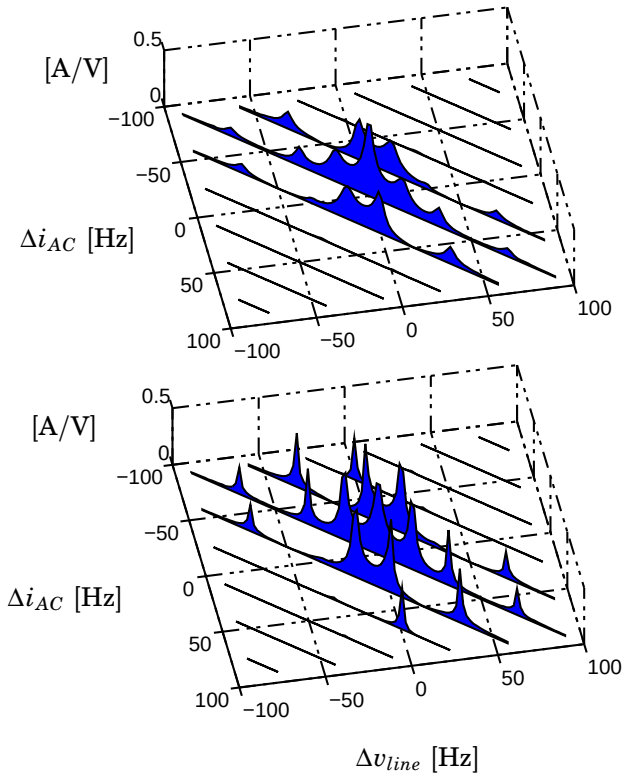

Figure 5. Plots showing the amplitude (A/V) of the coupling between the frequencies in Δv_{line} and Δi_{AC} for a single locomotive. The main diagonal is essentially the amplitude part of a Bode plot, a time-invariant model could only capture this part. The sub-diagonals show the transfer from one frequency to another. The load current is $i_{load} = 500\,\mathrm{A}$ in the upper plot and $i_{load} = -500\,\mathrm{A}$ in the lower plot illustrating the difference for a motor working as a load (driving) and as a generator (braking).

4. Conclusions and Future Work

Some of the possibilities of using periodic modeling of power systems have been shown. A model of a power converter was developed. It turned out to be a periodic gain matrix. This was used to model an inverter locomotive. The locomotive had a considerable frequency coupling, something that normally is not taken into account during controller design and stability analysis.

It was also shown how IQCs may be used in the analysis of systems with power converters. This could be further studied. Also it would be interesting to look at larger problems. For example interconnections of several locomotives running on the same net. Such systems must be very large in order to be realistic. This should require model reduction of time-periodic models which also is an interesting topic to be further studied.

5. References

Arrillaga, J., A. Medina, M. Lisboa, M. A. Cavia, and P. Sánchez (1994): "The harmonic domain. A frame of reference for power system harmonic analysis." *IEEE Trans. on Power Systems*, **10:1**, pp. 433–440.

Elmqvist, H., S. Mattsson, and M. Otter (1999): "Modelica - a language for physical system modeling, visualization and interaction." In *Proc. of the 1999 IEEE Symposium on Computer-Aided Control System Design*. Hawaii, USA.

Jönsson, U., C.-Y. Kao, and A. Megretski (1999): "Robustness analysis of periodic systems." In *Proceedings of 38th IEEE conference on Decisions and Control*. Phoenix, Arizona, USA.

Kundur, P. (1994): *Power System Stability and Control*. McGraw-Hill Inc., USA.

Megretski, A. and A. Rantzer (1997): "System analysis via integral quadratic constraints." *IEEE Transactions on Automatic Control*, **42:6**, pp. 819–830.

Meyer, M. (1999): "Netzstabilität in grossen Bahnnetzen." *Eisenbahn-Revue*, **7-8**, pp. 312–317.

Möllerstedt, E. and B. Bernhardsson (2000): "Out of control because of harmonics - an analysis of the harmonic response of an inverter locomotive." *IEEE Control Systems Magazine*, **20:4**, pp. 70–81.

Möllerstedt, E., A. Stothert, and H. Sandberg (2000): "Robust control of power converter." *To be submitted*.

Sandberg, H. and E. Möllerstedt (2000): "Harmonic modeling of the motor side of an inverter locomotive." In *Proceedings of the 9th IEEE Conference on Control Applications*. Anchorage, Alaska.

Stankovic, A., B. Lesieutre, and T. Aydin (1999): "Modeling and analysis of single-phase induction machines with dynamic phasors." *IEEE Transactions on Power Systems*, **14:1**, pp. 9–14.

Wereley, N. (1991): *Analysis and Control of Linear Periodically Time Varying Systems*. PhD thesis, Dept. of Aeronautics and Astronautics, MIT.

Willems, J. C. (1971): *The Analysis of Feedback Systems*. MIT Press, Cambridge, MA, USA.

Xu, W., J. Marti, and H. Dommel (1991): "A multiphase harmonic load flow solution technique." *IEEE Trans. on Power Systems*, **6:1**, pp. 174–182.

Paper 3

Harmonic Modeling of the Motor Side of an Inverter Locomotive

Henrik Sandberg and Erik Möllerstedt

Abstract

An AC-voltage source feeding an electric network results in a periodic excitation of the network. In steady state, all currents and voltages will be periodic with cycle time corresponding to the frequency of the voltage source. If the network is linear, all signals are sinusoidal and the network is solved using traditional methods. If the network contains components with nonlinear or switching dynamics, iterative methods based on harmonic balance are often required to obtain the periodic steady state solution.

By linearization of the system around the periodic solution, a linear time-periodic model is obtained. This can be used as a local description of the system in the neighborhood of the periodic solution. If only periodic signals are considered, a linearized model can be represented by a matrix, called the Harmonic Transfer Matrix (HTM).

The method is applied to the motor side of a modern inverter locomotive. Via the HTM, the steady-state response to constant or periodic disturbances or changes in reference values can be obtained.

1. Introduction

One example where traditional transfer function analysis has proven to be insufficient is in railway networks with modern inverter locomotives. These locomotives are equipped with voltage converters with high switching frequencies. The advantage compared to older locomotives include improved efficiency and less maintenance. There have been problems when these modern locomotives have been used with old power networks and signaling equipment. One historical example comes from Switzerland. During 1995 a power network resonance occurred which led to automatic shutdown of several inverter locomotives. Later studies showed that these locomotives were actually the cause of the incident. In some frequency bands the locomotives turned out to work more or less as *negative* resistors. One of these bands happened to overlap a network resonance frequency. At the time of the incident many older locomotives which normally damp the resonance were not in operation. Together these circumstances resulted in high amplitude current oscillations. This particular event is further described in [Meyer, 1999a].

A better understanding of the effects is thus wanted. There is an international research project named ESCARV (Electrical System Compatibility for Advanced Rail Vehicles), which has as goal to develop methods to test compatibility of rail networks, locomotives and signaling equipment. All the large train manufacturers in Europe, the Swiss and Italian railway companies and some universities are members in this project. The project should be finished in the end of year 2000. More information can be found in [Meyer, 1999a] and on `http://www.enotrac.com/escarv`.

To analyze these systems, time simulations or iterative methods like Harmonic Balance, see [Gilmore and Steer, 1991], often are used. Similar types of studies have been made under various names, Harmonic Power Flow Study in [Xia and Heydt, 1982], Unified Solution of Newton Type in [Acha *et al.*, 1989], and Harmonic Domain Algorithm in [Arrillaga *et al.*, 1994]. Unfortunately iterative methods are not guaranteed to converge and it is difficult to do stability and robustness analysis in time simulators. A method that avoids some of these problems was described in [Möllerstedt, 1998]. If a steady-state periodic solution is known it is possible to approximate the system as

a linear time-periodic system locally. A matrix called the Harmonic Transfer Matrix (HTM) describes how periodic signals interact in the neighborhood of the known solution.

In this paper a HTM of the motor side of an inverter locomotive is calculated and some typical results are shown. A similar model of a diode converter locomotives is made in [Möllerstedt and Bernhardsson, 2000a]. With the HTM it is possible to do detect dangerous cross-coupling of frequencies, and with some slight extensions to do stability and robustness analysis. This is not done here, see [Möllerstedt and Bernhardsson, 2000b; Möllerstedt and Bernhardsson, 2000a; Wereley, 1991] for more details.

Acknowledgments

We would like to thank Dr Markus Meyer at Adtranz Switzerland for giving us train models and advice. We would also like to thank Dr Andrew Paice at ABB Corporate Research Switzerland for working with us on this project and giving us the opportunity to work at the company.

2. Method

In this report all considerations will be made under steady state. This means all transients have died out and all quantities are constant or periodic. Periodic functions can be expanded into Fourier series with harmonic functions as basis. In the general case you need an infinite number of frequencies to expand a function, but in computer implementations you have to truncate after a finite number of terms. In practice this is sufficient, as the functions under consideration may often be approximated with just a few harmonics.

Let the periodic function have a fundamental frequency of ω_0 and the corresponding period T. The harmonics might be represented in complex form $e^{j\omega_0 t}$ or in real form $\sin \omega_0 t$ and $\cos \omega_0 t$ where $\omega_0 T = 2\pi$. Both representations have their advantages. In this article the complex form will be used. The Fourier series of a periodic function $v(t)$ is

$$v(t) = \sum_{k=-\infty}^{\infty} v_k e^{jk\omega_0 t}$$

where

$$v_k = \int_t^{t+T} v(\tau) e^{-jk\omega_0\tau} d\tau.$$

We are going to store the coefficients in a doubly-infinite frequency vector

$$\mathcal{V} = [\ \ldots\ \ v_{-2}\ \ v_{-1}\ \ v_0\ \ v_1\ \ v_2\ \ \ldots\ ]^T$$

If the series is truncated after N frequencies this leads to $(2N+1)$-dimensional vectors. If the function $v(t)$ is real then $v_{-k} = v_k^*$ where * denotes complex conjugate. Time-periodic vector and matrix functions will later also be expanded, and the same notation is used for them. The coefficients then have the same dimensions as the original function.

The relationship between input and output frequency vectors for a dynamical system under steady state is

$$\mathcal{J} = \boldsymbol{F}(\mathcal{V}), \quad \mathcal{J}, \mathcal{V} \in \boldsymbol{C}^{2N+1}$$

where F in general is a nonlinear vector function. F is normally cumbersome to derive and to use. The method of equating harmonics in an iterative way goes under the name *Harmonic Balance* and is reviewed in for example [Gilmore and Steer, 1991].

In [Möllerstedt, 1998] a way to go around the complicated procedure is presented. The idea is to make a linearization of F. If a steady-state solution, with frequency vectors $\mathcal{J}_0$ and $\mathcal{V}_0$, is known it can be used as a linearization point. Around this point the relationship between the frequency vectors $\mathcal{J}$ and $\mathcal{V}$ approximately can be written

$$\mathcal{J} = \mathcal{J}_0 + \mathcal{G}(\mathcal{V} - \mathcal{V}_0) \tag{1}$$

as a first-order Taylor expansion with

$$\mathcal{G} = \frac{\partial \mathcal{F}}{\partial \mathcal{V}} = \begin{bmatrix} \frac{\partial j_{-N}}{\partial v_{-N}} & \frac{\partial j_{-N}}{\partial v_{-N+1}} & \cdots & \frac{\partial j_{-N}}{\partial v_N} \\ \frac{\partial j_{-N+1}}{\partial v_{-N}} & \frac{\partial j_{-N+1}}{\partial v_{-N+1}} & \cdots & \frac{\partial j_{-N+1}}{\partial v_N} \\ \vdots & \vdots & \ddots & \vdots \\ \frac{\partial j_N}{\partial v_{-N}} & \frac{\partial j_N}{\partial v_{-N+1}} & \cdots & \frac{\partial j_N}{\partial v_N} \end{bmatrix}. \tag{2}$$

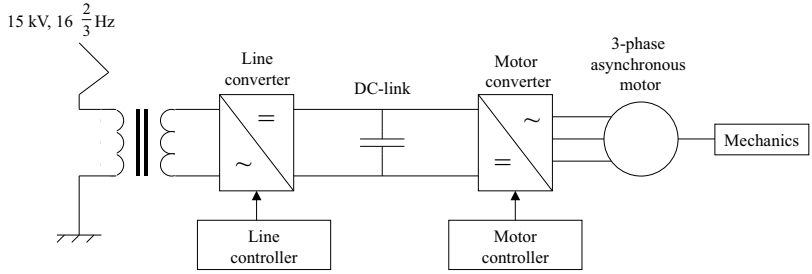

Figure 1. System overview of an inverter locomotive. The locomotive consists of two subsystems: the line and the motor side. They are connected with the DC-link. The method described in this article is applied to the motor side. Thus the effects on the motor and on the link from changing voltages in the DC-link and changing set points in the motor controller can be analyzed.

Here j_k are the coefficients of $\mathcal{J}$ and v_k are the coefficients of $\mathcal{V}$. $\mathcal{G}$ will in the following be called a Harmonic Transfer Matrix (HTM). The problems here are to find the linearization point and to evaluate the Jacobian (2). These things might be convenient to do through simulations or experiments, see [Möllerstedt, 1998]. The steady-state behavior of a Linear Time Periodic (LTP) system can be exactly described by a HTM, see [Wereley, 1991]. A Linear Time Invariant (LTI) system results in a HTM where only the main diagonal is non-zero, as there is no frequency coupling. The LTI-approximation of a modeled system is thus obtained by taking the main diagonal of the HTM.

3. System

A simple model of an AC-locomotive is shown in Figure 1. The locomotive is of general type propulsed by an Asynchronous Electrical Motor (ASM) fed through voltage converters. The converters are constructed with GTO-thyristors (Gate Turn-Off thyristors) or IGBTs (Insulated Gate Bipolar Transistor), high-voltage semiconductor switches. The technology is quite modern. It was not until the 80's this technology had its breakthrough and became economically efficient.

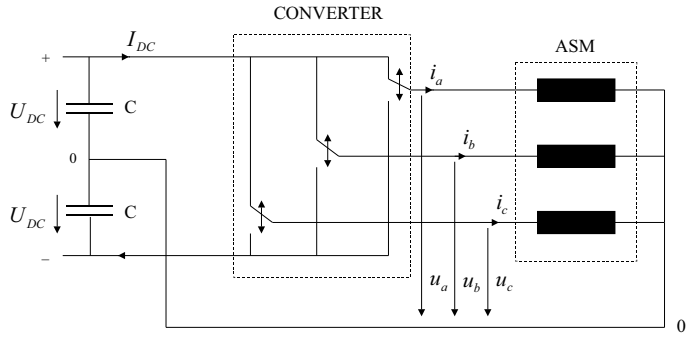

Figure 2. A simplified circuit describing the motor side of a converter locomotive. The currents and voltages are defined for the DC-link and the phases of the Asynchronous Electrical Motor (ASM). The three switches in the converter are displayed. The task of the controller is to switch these so that the magnetic flux in the motor moves on a circle and so that the correct mechanical torque is delivered.

The line voltage is first transformed down to a lower voltage and then fed to the line converter. The goals of the line controller is to keep a constant DC-link voltage and to draw a sinusoidal current from the line, in phase with the voltage to minimize reactive power. The instantaneous power into the locomotive from the line pulsates with the double net frequency, $33\frac{1}{3}$ Hz. The motor side on the other hand needs more or less constant instantaneous power. Therefore a capacitor and a filter is placed in the DC-link to compensate for the $33\frac{1}{3}$ Hz oscillation.

A motor converter is connected at the other end of the DC-link. This converter makes AC of variable frequency. The frequency must be variable in order to drive the engine at different speeds and torques. The motor converter and the engine are together called the motor side. The motor side is modeled in the following.

A good reference for learning more about trains in general is [Filipović, 1989]. For the network interaction issue of converter locomotives see [Meyer, 1999a] and [Meyer, 1999b].

Motor Converter

The converter is implemented with three switches, each one of them connected to one of the engine phases, see Figure 2. The converter switches the engine phases between $\pm U_{DC}$ to induce a sinusoidal motor flux of desired frequency.

The converter is modeled with a power balance where the power loss is neglected:

$$\begin{aligned} p_{DC}(t) &= 2U_{DC}(t)I_{DC}(t) \\ &= u_a(t)i_a(t) + u_b(t)i_b(t) + u_c(t)i_c(t) = p_{motor}(t). \end{aligned} \quad (3)$$

We now need to construct a frequency vector model of the converter. The power balance is a sum of terms which consist of multiplication of two time-periodic variables, voltage and current. Let us study the HTM of one of these terms and call the factors $u(t)$ and $i(t)$. Assume now each of them are perturbed by $\Delta u(t)$ and $\Delta i(t)$. Their product is then well approximated (small perturbations) by:

$$\Delta p(t) \approx i^0(t)\Delta u(t) + u^0(t)\Delta i(t) \quad (4)$$

where $u^0(t)$ and $i^0(t)$ are nominal periodic solutions. The error is here of second order. Notice that if the nominal solutions is constant this reduces to a classical linearization, otherwise we have multiplication with time-periodic factors. The HTM for a term in (4), generalized to apply for multi-dimensional inputs and outputs, is given in Lemma 1.

LEMMA 1—MULTIPLICATION WITH PERIODIC FUNCTION
Let all the signals in the vector-matrix multiplication

$$y(t) = A(t)x(t) \quad (5)$$

be periodic with the angular frequency ω_0. Equation (5) formulated with frequency vectors become

$$\mathcal{Y} = \mathcal{A}\mathcal{X}, \quad (6)$$

with the HTM (of Toeplitz structure)

$$\mathcal{A} = \begin{bmatrix} \ddots & \vdots & \vdots & \vdots & \\ \dots & A_0 & A_{-1} & A_{-2} & \dots \\ \dots & A_1 & A_0 & A_{-1} & \dots \\ \dots & A_2 & A_1 & A_0 & \dots \\ & \vdots & \vdots & \vdots & \ddots \end{bmatrix} \tag{7}$$

and the frequency vectors

$$\mathcal{X}^T = \begin{bmatrix} \dots & x_{-1}^T & x_0^T & x_1^T & \dots \end{bmatrix}$$
$$\mathcal{Y}^T = \begin{bmatrix} \dots & y_{-1}^T & y_0^T & y_1^T & \dots \end{bmatrix}.$$

Proof: By multiplication of the two complex Fourier series of $A(t)$ and $x(t)$ and equating the harmonics with $y(t)$ the relation is obtained:

$$\left(\sum_{k=-\infty}^{\infty} A_k e^{jk\omega_0 t}\right)\left(\sum_{i=-\infty}^{\infty} x_i e^{ji\omega_0 t}\right) = \sum_{k,i=-\infty}^{\infty} A_k x_i e^{j(k+i)\omega_0 t}$$
$$= \sum_{k=-\infty}^{\infty}\left(\sum_{i=-\infty}^{\infty} A_{k-i} x_i\right) e^{jk\omega_0 t} = \sum_{k=-\infty}^{\infty} y_k e^{jk\omega_0 t}.$$

□

By using (4) and Lemma 1 repeatedly in (3) we get a matrix relation between all the deviations of the voltages and currents if a nominal solution is given.

If the three-phase engine is a symmetric load it is enough to make the calculations with two variables. The three phases have a phase difference of 120° to one another. Therefore introduce the coordinate transformation $(a, b, c) \mapsto (\alpha, \beta)$. The new coordinates are stored as complex numbers:

$$\vec{x} = \frac{2}{3}\left(x_a e^{j0^\circ} + x_b e^{j120^\circ} + x_c e^{-j120^\circ}\right) = x_\alpha + j x_\beta \tag{8}$$

The equations in the following are expressed in these (α, β)-coordinates. The power for example becomes:

$$p_{motor}(t) = \frac{3}{2}(u_\alpha(t)i_\alpha(t) + u_\beta(t)i_\beta(t))$$

The power balance of the converter expressed in frequency vectors thus looks like

$$2(\mathcal{U}^0_{DC}\Delta I_{DC} + I^0_{DC}\Delta\mathcal{U}_{DC}) \\ = \frac{3}{2}(\mathcal{U}^0_\alpha\Delta I_\alpha + I^0_\alpha\Delta\mathcal{U}_\alpha + \mathcal{U}^0_\beta\Delta I_\beta + I^0_\beta\Delta\mathcal{U}_\beta) \quad (9)$$

where $\mathcal{U}^0$ and I^0 are Toeplitz matrices with the Fourier coefficients of the nominal voltage and currents solutions as elements, just as in Lemma 1. The α, β-variables are later going to be substituted.

Asynchronous Electrical Motor and Controller

On the right hand side of (9) we want to insert the ASM equations with the controller. In the following all the variables are given as complex numbers on the form $\vec{x} = x_\alpha + jx_\beta$, according to (8). In normalized quantities the ASM equations can be written as:

$$T^* \frac{d}{dt}\vec{\psi}_\mu(t) = n_0\,\vec{u}(t) - \rho\,\vec{\psi}_\mu(t) + \rho\,(1-\sigma)\vec{\psi}_r(t) \quad (10)$$

$$T^* \frac{d}{dt}\vec{\psi}_r(t) = (jn(t) - 1)\vec{\psi}_r(t) + \vec{\psi}_\mu(t) \quad (11)$$

and

$$m_{is}(t) = 2(\psi_{\mu\beta}(t)\psi_{r\alpha}(t) - \psi_{\mu\alpha}(t)\psi_{r\beta})(t),$$
$$n_s(t) = n_r(t) + n(t),$$
$$\vec{y}(t) = \frac{1}{1-\sigma}\vec{\psi}_\mu(t) - \vec{\psi}_r(t)$$

where $\vec{\psi}_\mu$ is the total flux, $\vec{\psi}_r$ the rotor flux, $\vec{u}$ the stator voltages, m_{is} the delivered mechanical torque, $\vec{y}$ the stator currents, n the mechanical motor frequency, n_s the electrical frequency and n_r the slip. All the

variables are normalized and have dimension [1]. n_0 is the so-called frequency ratio, ρ the time-constant ratio and σ the stray ratio, they are all motor parameters and are defined in [Sandberg, 1999]. There are other and more accurate models of ASMs. An introduction to ASMs is found in for example [McPherson and Laramore, 1990].

The fluxes are both rotating with the electrical frequency in the engine. This frequency normally differs from the mechanical frequency. The difference of the two is called the slip and is related to the delivered torque and to the angle between the fluxes. A positive slip results in a positive torque. When there is a negative slip the motor works as a brake and generates power which can be fed out to the line.

The engine is controlled by so-called indirect self control. Here this is modeled as multiplication of the measurable stator currents and the fluxes with a time-periodic gain, this feedback gives the applied stator voltages $\vec{u}$. A HTM of this is obtained with Lemma 1. In the implementation the continuous control signal is converted to switching signals by Pulse Width Modulation (PWM). This is modeled as a time lag of 1 ms corresponding to the switching frequency 250 Hz. See [Sandberg, 1999] for details.

There is a known sinusoidal solution to the engine equations. This is used as nominal solution. Now the engine-controller loop can be linearized and written on the form:

$$\dot{x}(t) = A(t)x(t) + B(t)u(t) \tag{12}$$
$$y(t) = C(t)x(t) + D(t)u(t) \tag{13}$$

where $A(t+T) = A(t)$ and analogously for $B(t)$, $C(t)$, $D(t)$, T is the electrical period. In this case the vectors contain

$$x(t) = [\Delta\psi_{\mu\alpha}\ \Delta\psi_{\mu\beta}\ \Delta\psi_{r\alpha}\ \Delta\psi_{r\beta}]^T$$
$$u(t) = [\Delta m_{sp}\ \ \Delta U_{DC}]^T$$
$$y(t) = [\Delta\psi_{\mu\alpha}\ \Delta\psi_{\mu\beta}\ \Delta y_{\alpha}\ \Delta y_{\beta}\ \Delta m_{is}]^T$$

where Δm_{sp} is the set point of the torque given to the engine controller. We want to derive a HTM between $u(t)$ and $y(t)$. This is obtained in Lemma 2. In the thesis [Wereley, 1991], linear time-periodic systems of this kind are studied and the result is taken from there.

LEMMA 2—[WERELEY, 1991]
The HTM $\mathcal{G}$ of a finite-dimensional linear time-periodic system as (12)–(13) is given by

$$\mathcal{Y} = \mathcal{G}\mathcal{U}$$

with

$$\mathcal{G} = \mathcal{C}(\mathcal{N} - \mathcal{A})^{-1}\mathcal{B} + \mathcal{D}$$

where $\mathcal{N} = \text{blkdiag}\{jn\omega_0 I\}$, $n \in Z$, and $\mathcal{A}, \mathcal{B}, \mathcal{C}, \mathcal{D}$ are block-Toeplitz matrices as in equation (7).

□

To connect the engine to the converter we can substitute these frequency vectors into (9).

4. Analysis of the System

Now we have HTMs of the engine-controller loop and the converter connection. It is then possible to plot different relations between inputs and outputs. If the main diagonal of a HTM is plotted, a sample of the Bode plot is obtained. If sub diagonals are present we can also study how frequencies interact. This enables a more powerful analysis.

As one input frequency can result in many output frequencies it is important that none of them excite a resonance in the system, in this case the DC-link is critical. Such studies can be made with HTMs.

It turns out in these examples that the sub diagonals often become zero when the nominal solution of the engine is pure sinusoidal. This is because the engine is a balanced three-phase load. When the engine is driven at higher speeds the frequency coupling is greater due to other controller strategies.

The Influence of the Set Point of the Torque on the DC-Link Current

Here the HTM to study the influence of m_{sp} on I_{DC} is constructed. In Figure 3 the linear time-invariant part (main diagonal) of the HTM is plotted. In fact the sub diagonals are zero in this case. The reason for this can be understood by studying the power of the engine. Under steady state the engine needs constant instantaneous power as the flux moves on a circle (perfect symmetric load). When a periodic

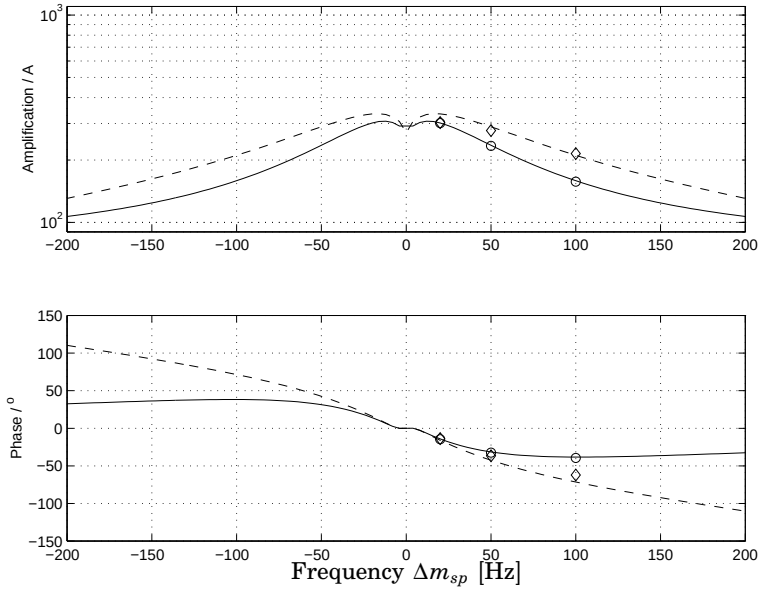

Figure 3. The amplitude and phase of the main diagonal of the HTM between ΔI_{DC} and Δm_{sp}. The solid line is from the HTM without PWM modeling and the dashed is with PWM modeling. The (◊) are from time simulations with PWM and (o) without PWM. It is seen that the PWM influences the transfer function for high frequencies.

perturbation is introduced the power will change with the same frequency. The DC-link voltage is assumed to be constant, and as input power equals output power the first-order approximation will be linear time invariant. If the DC-link voltage is assumed to be periodic, sub diagonals will arise due to the power balance.

Notice that the small time lag introduced by the PWM results in quite large changes for higher frequencies.

The influence of the Set Point of the Torque on the Stator Current

Here the relationship between the torque set point and the stator current in the motor will be shown. In Figure 4 time-domain results are plotted for one fundamental period. The input is a pure cosine of fre-

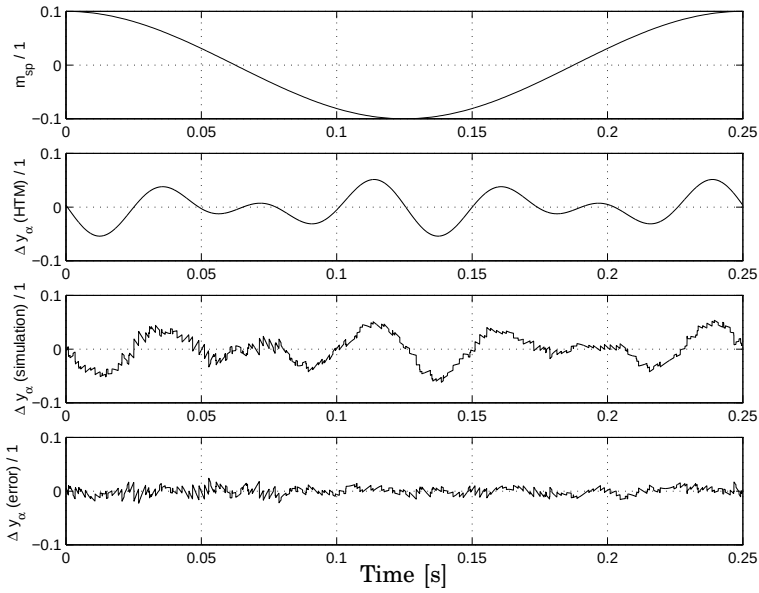

Figure 4. The time-domain appearance of one fundamental period, T, of the normalized stator current Δy_α. At the top the input is displayed. It is followed by the result from the HTM-model, the simulated result, and the difference of the two. It is seen that the modeling is accurate for low frequencies. The high frequency ripple is outside the studied range.

quency 4 Hz and in the output there are two frequencies, 8 and 32 Hz. When compared to time-domain simulations it is seen that the low frequency parts are almost perfectly modeled. The high frequency ripple from the converter is not captured with this model, it is outside the studied frequency range.

The Admittance Matrix of the Motor Side

Here a so-called admittance matrix will be plotted. We want to study the behavior of the entire motor side as seen from the DC-link for some operating point of the engine. This means to find the relationship of how ΔU_{DC} influences ΔI_{DC}. The admittance matrix can be used to connect the motor side with a similar line side model. The motor side

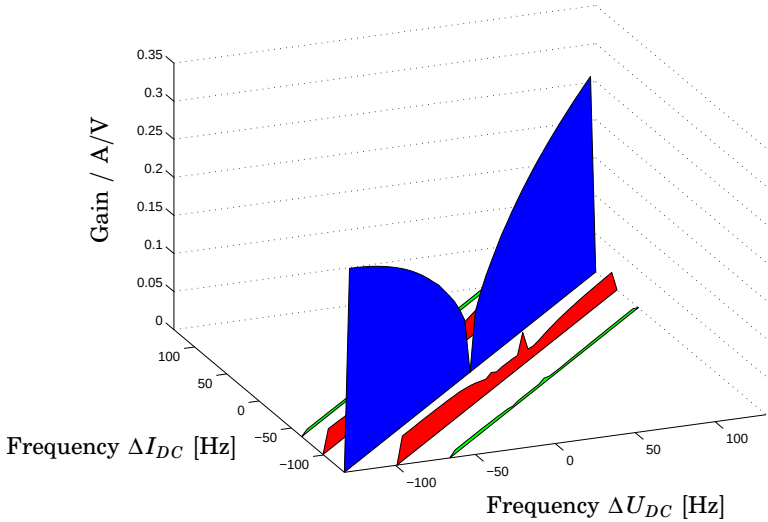

Figure 5. The absolute values of the admittance (HTM) matrix for the motor side of an inverter locomotive. That is the relation between current and the voltage in the DC-link. The locomotive is operating with a constant torque with small 33 Hz oscillations in U_{DC}. The main diagonal is dominating, which means that the motor side is mainly linear time-invariant at this operating point. The distance between the sub diagonals is 33 Hz.

is linearized around a periodic trajectory with small 33 Hz oscillations in the DC-link and the motor delivering a constant torque. This is a conceivable operating point, as the energy pulsates into the DC-link from the line side converter with the double line frequency.

The absolute values of the HTM is shown in Figure 5. The main diagonal is strongly dominating here. So a linear time-invariant model seems to be able to model most of the dynamics. If there were no oscillations in the DC-link at the operating point, no sub diagonals would be present. An operating point with larger oscillations would give larger sub diagonals. This is a consequence of the symmetries in the model and the control technique.

The main diagonal alone is plotted in Figure 6 (solid line) in a Bode diagram. From this we see that the motor side is an inductive

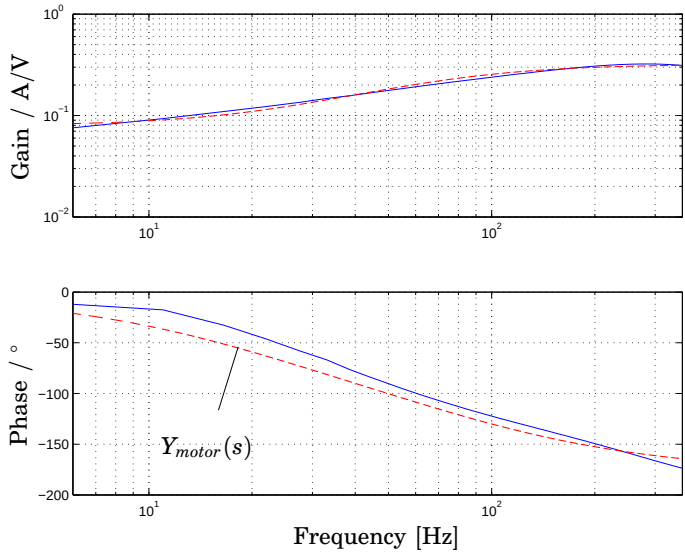

Figure 6. Here the amplitude and phase of the main diagonal of the admittance matrix in Figure 5 are displayed in a wider frequency range (solid line). For frequencies above 50 Hz the phase plot indicates that the motor side works as an active load (negative resistance) to the DC-link. This might inflict stability problems when the line side is included in the model. A first-order transfer function, $Y_{motor}(s)$, fits the main diagoal well (dashed line). This is a non-minimum phase system.

load to the link and that for frequencies above 50 Hz it has negative resistance. This means the motor side supplies the link with energy for high frequencies, which could be problematic from a stability point of view. We also see from the relationship of the amplitude and the phase that there seems to be a zero in the right half plane, i.e. the motor side is non-minimum phase. Such systems are known to be inherently hard to control. By simple curve fitting we see that a first-order transfer function

$$Y_{motor}(s) = -0.32 \cdot \frac{s-20}{s+80} \qquad [\mathrm{A/V}] \tag{14}$$

fits the main diagonal well (dashed line). For a simplified analysis of

the motor side this model could be used.

The non-minimum phase behavior can be understood as the motor is controlled to deliver a constant torque. When the voltage level rises in the DC-link, the current must decrease in order to keep the power input to the motor constant. There is, however, a feedforward loop from the DC-link voltage to the motor controller that raises the torque set point, in order to help the line side controller in the stabilization of the DC-link. This only works for low frequencies.

5. Conclusions and Future Work

In this article we have studied harmonic transfer matrices and have shown how to use them to model systems with switching components. The method was exemplified on an inverter locomotive. In particular, a simplified model of the admittance of the motor side was developed.

The HTMs are useful to describe periodic systems. They give a compact description and are easy to interpret. With the HTM it is possible to answer a wider range of questions than it is possible to with traditional analysis. Particularly frequency interaction is described, which is often seen in nonlinear systems with periodic trajectories.

A generalization of the HTM described here, is the Harmonic Transfer Function (HTF), see [Möllerstedt and Bernhardsson, 2000a; Wereley, 1991; Möllerstedt and Bernhardsson, 2000b]. There exist a Nyquist criterion for the HTF which enables stability and robustness studies. There are many analogies between the HTF and the transfer function for LTI systems, future work would include transferring more results from LTI theory.

6. References

Acha, E., J. Arrillaga, A. Medina, and A. Semlyen (1989): "General frame of reference for analysis of harmonic distortion in systems with multiple transformer nonlinearities." *IEE Proceedings*, **136C:5**, pp. 271–278.

Arrillaga, J., A. Medina, M. Lisboa, M. A. Cavia, and P. Sánchez (1994): "The harmonic domain. A frame of reference for power system harmonic analysis." *IEEE Trans. on Power Systems*, **10:1**, pp. 433–440.

Filipović, Ž. (1989): *Elektrische Bahnen*. Springer-Verlag. ISBN 0-387-51121-0.

Gilmore, R. and M. Steer (1991): "Nonlinear circuit analysis using the method of harmonic balance - A review of the art. Part i. Introductory concepts." *Int J. Microwave and Millimeter-Wave Computer-Aided Eng.*, **1:1**, pp. 22–37.

McPherson, G. and R. Laramore (1990): *An introduction to electrical machines and transformers*. John Wiley & Sons. ISBN 0-471-63529-4.

Meyer, M. (1999a): "Netzstabilität in grossen Bahnnetzen." *Eisenbahn-Revue*, **7-8**, pp. 312–317.

Meyer, M. (1999b): "Über das Netzverhalten von Umrichterlokomotiven." *Eisenbahn-Revue*, **8-9**, pp. 241–274.

Möllerstedt, E. (1998): "An aggregated approach to harmonic modelling of loads in power distribution networks." Technical Report Licentiate thesis ISRN LUTFD2/TFRT–3221–SE. Department of Automatic Control, Lund Institute of Technology, Sweden.

Möllerstedt, E. and B. Bernhardsson (2000a): "A harmonic transfer function model for a diode converter train." In *IEEE Power Engineering Society Winter Meeting, Singapore*.

Möllerstedt, E. and B. Bernhardsson (2000b): "Out of control because of harmonics – an analysis of harmonic response of an inverter train." *Control Systems Magazine*.

Sandberg, H. (1999): "Nonlinear modeling of locomotive propulsion system and control." Technical Report Masters thesis ISRN LUTFD2/TFRT–5625–SE. Department of Automatic Control, Lund Institute of Technology, Sweden.

Wereley, N. (1991): *Analysis and Control of Linear Periodically Time Varying Systems*. PhD thesis, Dept. of Aeronautics and Astronautics, MIT.

Xia, D. and G. Heydt (1982): "Harmonic power flow studies, part I - formulation and solution, part II - Implementation and practical aspects." *IEEE Transactions on Power Apparatus and Systems*, **101:6**, pp. 1257–1270.